Published in final edited form as:
Mol Microbiol. 2013 September ; 89(5): 929–948. doi:10.1111/mmi.12321.

Genetic Analysis of *Agrobacterium tumefaciens* Unipolar Polysaccharide Production Reveals Complex Integrated Control of the Motile-to-Sessile Switch

Jing Xu[1], **Jinwoo Kim**[2], **Benjamin J. Koestler**[3], **Jeong-Hyeon Choi**[4,†], **Christopher M. Waters**[3], and **Clay Fuqua**[1,*]

[1]Department of Biology, Indiana University, Bloomington, IN 47405

[2]Division of Applied Life Science, Gyeongsang National University, Jinju 660-701, Korea

[3]Department of Microbiology and Molecular Genetics, Michigan State University, East Lansing, MI 48824

[4]Center for Genomics and Bioinformatics, Indiana University, Bloomington, IN

Summary

Many bacteria colonize surfaces and transition to a sessile mode of growth. The plant pathogen *Agrobacterium tumefaciens* produces a unipolar polysaccharide (UPP) adhesin at single cell poles that contact surfaces. Here we report that elevated levels of the intracellular signal cyclic diguanosine monophosphate (c-di-GMP) lead to surface-contact-independent UPP production and a red colony phenotype due to production of UPP and the exopolysaccharide cellulose, when *A. tumefaciens* is incubated with the polysaccharide stain Congo Red. Transposon mutations with elevated Congo Red staining identified presumptive UPP negative regulators, mutants for which were hyperadherent, producing UPP irrespective of surface contact. Multiple independent mutations were obtained in *visN* and *visR*, activators of flagellar motility in *A. tumefaciens*, now found to inhibit UPP and cellulose production. Expression analysis in a *visR* mutant and isolation of suppressor mutations, identified three diguanylate cyclases inhibited by VisR. Null mutations for two of these genes decrease attachment and UPP production, but do not alter cellular c-di-GMP levels. However, analysis of catalytic site mutants revealed their GGDEF motifs are required to increase UPP production and surface attachment. Mutations in a specific presumptive cyclic diguanosine monophosphate phosphodiesterase also elevate UPP production and attachment, consistent with c-di-GMP activation of surface-dependent adhesin deployment.

Keywords

Attachment; Unipolar polysaccharide; Cellulose; Congo Red; VisN-VisR; Biofilm; Motility; c-di-GMP

Introduction

Bacteria can exist as either free-swimming single cells or attached to surfaces and sessile (Pratt & Kolter, 1998). The transition from a motile to sessile mode of growth is often coupled with termination of flagellar motility and activation of exopolysaccharide

*Address for correspondence: Clay Fuqua, Dept. Biol., 1001 E. 3rd St., Jordan Hall 142, Indiana Univ., Bloomington, IN 47405-1847. Tel: 812-856-6005, FAX: 812-855-6705, cfuqua@indiana.edu.
†Current address: Molecular Oncology Program, Georgia Regent's University, Augusta GA 30912

production (Branda *et al.*, 2005, Li *et al.*, 2012, Blair *et al.*, 2008). Bacterial attachment can lead to biofilm formation, which is typified by the production of a self-secreted extracellular matrix composed of exopolysaccharides, proteins, lipids and sometimes DNA (Cogan & Keener, 2004, Danhorn & Fuqua, 2007, Kolter & Greenberg, 2006). The motile-to-biofilm switch is influenced by environmental cues and impacts antibiotic resistance, bacterial dispersion, and disease persistence (Mah *et al.*, 2003, Danhorn & Fuqua, 2007, Hall-Stoodley *et al.*, 2004).

In many bacteria the intracellular signal cyclic diguanosine monophosphate (c-di-GMP) has emerged as a major determinant of whether cells favor motility or attachment (D'Argenio & Miller, 2004). The general trend is that elevated c-di-GMP levels promote polysaccharide biosynthesis and biofilm formation while impeding the synthesis of flagella and swimming motility (Hengge, 2009). Cellular pools of c-di-GMP are inversely controlled by diguanylate cyclases (DGCs) and phosphodiesterases (PDEs) (Hengge, 2009). DGCs contain a conserved GGDEF domain and catalyze synthesis of c-di-GMP molecules while PDEs contain either an EAL or HD-GYP domain and drive degradation of the signal molecules (Simm *et al.*, 2004, Ryan *et al.*, 2006). Many bacterial genomes encode multiple proteins with GGDEF and EAL domains, and at some frequency both motifs are found on the same protein. In addition, these proteins often also contain additional regulatory motifs such as HAMP and PAS domains, suggesting that they respond to environmental stimuli to control c-di-GMP levels (Tamayo *et al.*, 2007).

Recent work has revealed distinct mechanisms by which c-di-GMP regulates the motile-to-sessile transition in different bacteria. Intracellular c-di-GMP controls activities that promote surface colonization including the elaboration of adhesin proteins, diminishing flagellar locomotion and exopolysaccharide synthesis (Ryan et al., 2006). The response to c-di-GMP can be transduced by a variety of receptors including riboswitches and several different classes of proteins, most notably those with PilZ-type domains, but also others. These effectors can control transcription or impart direct allosteric regulation of target processes. One of the most comprehensively studied systems is in the dimorphic Alpha-proteobacterium *Caulobacter crescentus* for which c-di-GMP plays an important role in controlling cellular differentiation from a motile, flagellated swarmer cell to a non-motile and often adherent stalked cell (Brown *et al.*, 2009). Two active DGC proteins DgcB and PleD physically localize to the incipient stalk pole, and in parallel with inactivation of PDE proteins, drive a localized c-di-GMP increase, which stimulates stalk morphogenesis and entry of the cell into the S phase of active DNA replication (Abel *et al.*, 2011). This control is in part mediated by association of c-di-GMP with an enzymatically inactive DGC homologue called PopA, and possibly additional effectors (Duerig *et al.*, 2009).

Agrobacterium tumefaciens is a pathogen that causes crown gall disease on plants due to its ability to transfer a segment of its own DNA into nucleus of plant cells where it integrates into host cell chromosomes (Van Larebeke *et al.*, 1974, Watson *et al.*, 1975). *A. tumefaciens* is a member of the *Alphaproteobacteria* as is *C. crescentus*, and although it is rod-shaped, also exhibits asymmetric cell division (Brown *et al.*, 2012). An early step in *A. tumefaciens* pathogenesis is attachment to host plants, which can subsequently lead to biofilm formation (Douglas *et al.*, 1982, Matthysse, 1986). We have observed that a unipolar polysaccharide (UPP) is produced at a single pole of *A. tumefaciens* cells that contact surfaces during adhesion but this structure is rarely observed in planktonic cells or in colonies on solid media (Li et al., 2012, Xu *et al.*, 2012). Therefore, the production of UPP is a landmark for permanent attachment and transitioning into the sessile polar attachment stage. Investigating UPP regulation should shed light on how bacterial cells sense and respond to surface contact and provide insights on the motile-to-sessile transition.

In this study, we first show that cells with elevated intracellular c-di-GMP levels produce the UPP independent of surface contact. Extending these findings we have isolated mutants that manifest misregulation of UPP synthesis and suppressors of these mutants that reverse this phenotype. Among mutants with altered c-di-GMP levels we have found that the VisN-VisR transcriptional regulators play a key role in regulating attachment, functioning to control motility while repressing the production of UPP and cellulose through modulating c-di-GMP levels. VisN and VisR impart a profound influence over the motile-to-sessile transition in *A. tumefaciens* at least in part through influencing c-di-GMP pools.

Results

Ectopic expression of a diguanylate cyclase homologue stimulates aggregation and UPP production

In many different bacteria, GGDEF proteins and c-di-GMP often control production of polysaccharides (Hengge, 2009). The PleD protein of *Caulobacter crescentus* was the first GGDEF protein for which diguanylate cyclase activity was demonstrated *in vitro* (Abel et al., 2011). PleD consists of tandem response regulator receiver domains and a GGDEF effector domain (Fig. S1), through which phosphorylation regulates c-di-GMP synthesis in *C. crescentus* (Aldridge *et al.*, 2003). Well prior to the recognition of the widespread role for c-di-GMP, it was reported that synthesis of cellulose *in vitro* with a crude cellulase enzyme preparation from *A. tumefaciens* was strongly stimulated by c-di-GMP (Amikam & Benziman, 1989). During examination of specific *Caulobacter* homologues in *A. tumefaciens* (Kim, 2013), we observed that expression of a plasmid-borne *pleD* homologue (Atu1297, P_{lac}-*pleD*) in an otherwise wild-type *A. tumefaciens* C58 resulted in a high frequency of large aggregates in colonies grown on solid medium (Fig. 1A) and similarly in planktonic cultures (Fig. S2A). These aggregates stained copiously with fluorescently tagged wheat germ agglutinin (fl-WGA), which labels a presumptive *N*-acetyl glucosamine (GlcNAc) component of the UPP. Ectopic expression of *pleD* in an otherwise wild type strain also strongly elevated biofilm formation (Fig. 1B), suggesting increased levels of adhesive polysaccharides. However, in-frame deletion of *pleD* in an otherwise wild type strain did not diminish biofilm formation (Kim, 2013).

PleD-dependent phenotypes require the exopolysaccharides cellulose and UPP

Production of β-linked polysaccharides in colonies can often be visualized by growth in the presence of specific stains. The visible dye Congo Red stains colonies that produce specific polysaccharides (also in some cases amyloid proteins, (Howie & Brewer, 2009)), and the intensity of red staining is proportional to the amount of Congo Red-reactive polysaccharide produced (Romling, 2005). Growth under inducing conditions for *A. tumefaciens* harboring the P_{lac}-*pleD* plasmid resulted in dark red staining on ATGN minimal medium with Congo Red (ATGN-CR) relative to the non-induced conditions (Fig. 1C). We designate this as the Elevated Congo Red (ECR) phenotype and will discuss it further below. The ECR phenotype suggested elevated polysaccharide production in *A. tumefaciens* due to P_{lac}-*pleD* expression.

A. tumefaciens is recognized to produce several different exopolysaccharides including succinoglycan, β-1,2 glucan, β-1,3 glucan, cellulose and UPP. Independent and combinatorial mutational analysis of these different polysaccharides revealed that the UPP was strictly required for attachment (Xu et al., 2012), whereas the others were not required. Examination of these exopolysaccharide mutants expressing the P_{lac}-*pleD* plasmid and grown on Congo Red revealed that either UPP or cellulose could suffice for the ECR phenotype, and that mutational disruption of both pathways was required to significantly

diminish the intense Congo Red staining (Fig. 1C). None of the other exopolysaccharide mutants were affected for the PleD-stimulated ECR phenotype (Fig. S2B).

Induction of *pleD* expression in Δ*cel* mutants resulted in small aggregates and rosettes in colonies on solid medium, which were extensively labeled with fl-WGA (Fig. 1A). Expression of *pleD* in Δ*upp* mutants also drove aggregate formation in colonies, but in contrast these were fragile clusters without rosettes and seldomly labeled with fl-WGA. Strikingly, mutants with both Δ*cel* Δ*upp* deletions did not aggregate and revealed single cells with no visible fl-WGA staining (Fig. 1A). These findings suggest that ectopic *pleD* expression stimulates increased production of UPP and cellulose, both of which contribute to increased cellular aggregation.

Wild type C58 expressing the P_{lac}-*pleD* plasmid exhibits elevated biofilm formation (Fig. 1B). The profound biofilm deficiency of the Δ*upp* mutant could not be rescued by plasmid-borne *pleD*, and this was also true in the Δ*upp*Δ*cel* mutant (Fig. 1B). The Δ*cel* mutation alone significantly diminished PleD-stimulated biofilm formation, but this remained substantially greater than the plasmid free derivative (Fig. 1B). Although mutation of the *cel* genes does not substantially impact biofilm formation at native levels of *pleD* expression, elevated cellulose production in response to ectopic *pleD* expression clearly contributes to biofilm formation (Fig. 1B).

PleD of A. tumefaciens is a diguanylate cyclase that drives c-di-GMP synthesis

To test whether the plasmid borne *pleD* homologue elevates c-di-GMP, we measured intracellular levels of the signal molecule using liquid chromatography coupled with tandem mass spectrometry (LC-MS/MS). The intracellular c-di-GMP concentration of the *A. tumefaciens* wild type strain is approximately 50–100 nM. The same strain harboring the P_{lac}-*pleD* plasmid is approximately 66 fold higher than that observed in the absence of the plasmid (Fig. 1D). Site-specific mutation of the plasmid-borne *pleD* GGEEF motif (Fig. S1B, the putative catalytic site for diguanylate cyclases) to GGAAF (*pleD**) abolished its ability to cause the ECR phenotype (Fig. 1E) and correspondingly decreased c-di-GMP levels to near wild type levels (Fig. 1D). Expression of the *pleD* plasmid in *Escherichia coli* DH5α (a heterologous host without other *A. tumefaciens* proteins and low basal c-di-GMP) also resulted in a striking increase in c-di-GMP when *pleD* expression was induced (46 fold over the same strain without the plasmid), and this increase was abolished in the GGAAF *pleD** mutant (Fig. 1D). Taken together, these observations suggest that ectopic expression of *pleD* stimulates its DGC activity, increasing c-di-GMP levels in *A. tumefaciens* and elevating synthesis of both cellulose and UPP polysaccharides. In turn this results in the ECR phenotype and enhanced biofilm formation.

A genetic screen for transposon mutants that mimic ectopic pleD expression

With our understanding of the genetic basis for the ECR colony phenotype a forward genetic screen was implemented to systematically explore how production of the UPP polysaccharide is regulated (Fig. S3A and S3B). To avoid the influence of other EPSs (particularly cellulose) we used a C58 derivative genetically disabled for the synthesis of all major EPSs (succinoglycan, β-1,2 glucan, β-1,3 glucan and cellulose) except for UPP (this mutant was designated as $EPS^{-}UPP^{+}$). We reasoned that mutation of a negative regulator that would increase UPP production in colonies grown on ATGN-CR solid medium should phenocopy the ECR phenotype exhibited by strains ectopically expressing *pleD*. Mutagenesis of the $EPS^{-}UPP^{+}$ mutant with the *Mariner* transposon was performed, and greater than 25,000 colonies were screened on ATGN-CR plates, yielding a collection of mutants with the ECR phenotype. Mutants with elevated Congo Red binding (ECR mutants) were incubated with fl-WGA and observed under fluorescence microscopy to visualize UPP

production. All ECR mutants exhibited notable production of UPP both in colonies (Fig. S3C) and in planktonic cultures (data not shown). The sites of transposon insertion were sequenced in these mutants and multiple independent disruptions were found in four discrete loci (initially designated as ECR1, ECR2, ECR3 and ECR4). Transposon insertions in Atu1130 and Atu1631, encoding a short chain dehydrogenase homologue (ECR2 class, three mutants) and a CheY single domain type response regulator (ECR3 class, six mutants) respectively, resulted in the ECR phenotype, but the basis for these mutant phenotypes remain unclear and they require additional analysis. The remaining two classes of mutants (ECR1 and ECR4) were examined further in this study.

VisN and VisR inversely regulate swimming and UPP-mediated biofilm formation

The ECR1 class of mutants was due to disruptions of two linked genes Atu0524 and Atu0525 (Fig. 2A), in which seven independent mutants were isolated. These genes are annotated in the *A. tumefaciens* genome as LuxR-FixJ type transcriptional regulators (Fig. 2B) and are highly homologous to *visN* and *visR* (vital in swimming), reported to control motility in *Sinorhizobium meliloti* and other rhizobia (Sourjik *et al.*, 2000). The *visN* and *visR* genes form a presumptive two-gene operon and are located between the chemotaxis and flagellar gene clusters on the *A. tumefaciens* C58 circular chromosome. The *visN* and *visR* gene products share similarity within their C-terminal regions with the DNA binding domains of LuxR and FixJ homologues, as well as to each other (Fig. 2B). However, the N-terminal sequences of VisN and VisR do not resemble either the acylhomoserine lactone binding motif of LuxR homologues nor the phosphate-receiver domain of FixJ. The N-termini of VisN and VisR also do not resemble each other.

Mutations in *visN* and *visR* cause a loss of motility in *S. meliloti* due to failure to express flagellar genes (Sourjik et al., 2000). The *A. tumefaciens* transposon mutants in *visN* or *visR* were also non-motile (Fig. S4A). The transposon mutants described above were isolated in the $EPS^{-}UPP^{+}$ parent background, which exhibited a moderate decrease of biofilm formation and swimming motility relative to wild type because of one of the deleted polysaccharide gene clusters, *chvAB*, mutants of which are highly pleiotropic (Xu et al., 2012). Transposon insertions in *visN* might also be polar on downstream *visR.* We therefore generated individual site-specific, in-frame deletions of *visN* and *visR* genes in the original $EPS^{-}UPP^{+}$ parent and in the wild type. The $EPS^{-}UPP^{+}$ *visN* and *visR* deletion mutants exhibited phenotypes identical to the transposon mutants and to each other, and were non-motile (Fig. S4A). Both mutants exhibited elevated biofilm formation (Fig. S4C), even with the loss of swimming motility (known to diminish attachment efficiency (Merritt *et al.*, 2007)). The Δ*visN* and Δ*visR* mutants also exhibited elevated UPP production in both colonies and planktonic phase (Fig. S4D).

The Δ*visN* and Δ*visR* mutations in the wild type resulted in phenotypes consistent with the $EPS^{-}UPP^{+}$ background. However, in colonies (Fig. 3C) and liquid medium (Fig. 2C) they formed very large aggregates with extensive UPP staining. On solid medium with Congo Red (ATGN-CR) Δ*visN* and Δ*visR* mutants had red ECR colony phenotypes (Fig. 2D). The Δ*visN* and Δ*visR* mutants were elevated for biofilm formation compared to the wild type (Fig. 2E).

Ectopic expression of visN and visR

Both the *visN* and *visR* deletion mutants grown on ATGN-CR medium were complemented by the corresponding plasmid-borne gene expressed from P_{lac} (Fig. 2D). Biofilm formation was in fact inhibited to below wild type levels by the individual *visN* and *visR* plasmids and a plasmid expressing both *visN* and *visR* caused the strongest inhibition (Fig. 2E). The Δ*visN* and Δ*visR* mutants were also fully complemented to wild type motility by these

plasmids (Fig. S5A). Neither mutation was rescued by provision of the other gene (e.g. *visN* mutation with plasmid-borne *visR)* in terms of swimming motility or Congo Red staining, but a plasmid expressing both *visN* and *visR* corrected either mutant for both of these phenotypes (Fig. S5). This suggests that VisN and VisR play discrete roles in regulating the motile-to-sessile switch.

Cellulose and UPP both contribute to the visR mutant phenotypes

The Δ*visR* mutant was chosen for further investigation since the Δ*visN* and Δ*visR* mutants phenocopy each other. To test whether the *visR* mutant phenotypes require UPP and cellulose, we constructed Δ*visR*Δ*upp*, Δ*visR*Δ*cel* double mutants and a Δ*visR*Δ*cel*Δ*upp* triple mutant. The Δ*visR*Δ*upp* mutant retained an ECR phenotype similar to Δ*visR.* The Δ*visR*Δ*cel* mutant was faintly redder than wild type, although significantly lighter than Δ*visR* (Fig. 3A). These data suggest the ECR phenotype of the Δ*visR* mutant in the otherwise wild type background is substantially due to cellulose overproduction, and to a lesser extent due to UPP overproduction (although in the original screen with the $EPS^{-}UPP^{+}$ parent, the ECR phenotype was due to UPP alone). The ECR phenotype was largely abolished in the Δ*visR*Δ*cel*Δ*upp* mutant (Fig. 3A), reflecting the participation of both polysaccharides.

The Δ*visR* mutant also was elevated for biofilm formation, and both cellulose and UPP contributed to this phenotype. The Δ*visR*Δ*cel* mutant was decreased for biofilm formation, revealing a role for cellulose in the increased biofilm formation of the Δ*visR* mutant (Fig. 3B). Consistent with our observation that UPP is essential for biofilm formation, the Δ*visR*Δ*upp* mutant and Δ*visR*Δ*cel*Δ*upp* mutant were completely unable to form biofilms (Fig. 3B). The Δ*visR* mutant formed large aggregates in colonies, which were copiously labeled by fl-WGA (Fig. 3C). The Δ*visR*Δ*cel* mutant formed UPP--dependent small aggregates and rosettes in colonies, which were extensively labeled with fl-WGA. The Δ*visR*Δ*upp* mutant formed weakly associated, cellulose-dependent aggregates, which were seldomly labeled with fl-WGA (Fig. 3B). In contrast, Δ*visR*Δ*cel*Δ*upp* mutants did not aggregate and revealed single cells with no visible fl-WGA staining. Overall, these findings suggest that both elevated UPP and increased cellulose production in the Δ*visR* mutant drive cellular aggregation, enhance biofilm formation and contribute to the ECR phenotype.

UPP visualization with electron microscopy

Scanning electron microscopy (SEM) and transmission electron microscopy (TEM) revealed production of the UPP. To limit large aggregates due to cellulose that might obscure the UPP structure, the $EPS^{-}UPP^{+}$Δ*visR* strain was used for electron microscopy. In contrast to wild type cells or $EPS^{-}UPP+$ cells, EPS^{-}Δ*visR* mutants produced UPP in planktonic phase, thereby allowing it to be visualized more readily by electron microscopy. Scanning electron microscopy (SEM) revealed rosette formation (cellular aggregates due to adhesion between cells at their poles) and a consistent unipolar protrusion in EPS^{-}Δ*visR* mutants (Fig. 4A). This protrusion varied from a small unipolar bulb of material or a more extended, fibrillar material. The material was not visible on any cells of the EPS^{-}Δ*visR* mutant with a transposon insertion in *uppE* (Fig. 4A), one of UPP biosynthesis genes ((Xu et al., 2012)). Using TEM, unipolar fibers from the $EPS^{-}UPP^{+}$Δ*visR* mutant were also decorated with colloidal gold-labeled WGA, whereas no polar labeling was observed for UPP^{-} strains (Fig. 4B).

A specific diguanylate cyclase homologue dgcA is required for elevated UPP in the ΔvisR mutant

To further investigate how *visN* and *visR* exert their function in UPP control, we performed a genetic screen for suppressors by mutagenizing the $EPS^{-}UPP^{+}$Δ*visR* mutant with the *Mariner* transposon to identify mutants with Decreased Congo Red binding (DCR) (Fig.

S3A and B). As expected, we identified several UPP biosynthesis genes (Xu et al., 2012). In addition, three independent mutants were isolated with transposon insertions in Atu1257, encoding a putative GGDEF-type diguanylate cyclase homologue (designated *dgcA*) with seven predicted transmembrane domains (Fig. S1). In-frame deletion of *dgcA* in the EPS$^-$UPP$^+$Δ*visR* mutant abolished the ECR phenotype and diminished UPP dysregulation, and these phenotypes could be complemented by providing a plasmid-borne P_{lac}-*dgcA* (Fig. 5). This P_{lac}-*dgcA* plasmid also resulted in elevated CR binding and UPP production in the EPS$^-$UPP$^+$ mutant (Fig. 5).

DNA microarray analysis of the VisR transcriptome

To provide additional insights into how VisNR exerts control on biofilm formation and motility, a DNA microarray experiment was performed to compare the transcriptional profile of the Δ*visR* mutant and the wild type. Expression data showed that genes with decreased expression in the *visR* mutant and thus under presumptive VisR positive control included flagellar and chemotaxis genes as well as the transcription factor *rem* (Rotter *et al.*, 2006), and the *imp* genes (Wu *et al.*, 2012) encoding a Type VI secretion system (Table S1, Fig. 6A). Although several exopolysaccharide synthesis genes were also down in the *visR* mutant (Fig. 6A), none of these are UPP or cellulose biosynthetic genes (Xu et al., 2012, Matthysse *et al.*, 1995). A smaller number of genes were increased in expression in the *visR* mutant and therefore under presumptive VisR-dependent repression (Table S2), including a pair of genes encoding putative DGC proteins, Atu1691 (renamed as *dgcB*) and Atu2179 (renamed as *dgcC*). Similar to DgcA, DgcC is predicted to be a membrane-associated protein, whereas DgcB is predicted to be cytoplasmic (Fig. S1). Notably, *dgcA* expression was not elevated in the Δ*visR* mutant.

To confirm the microarray data, plasmid-borne promoter translational fusions with *lacZ* were constructed with the upstream regions of Atu0573 (*rem*), Atu0560 (*motA*) and Atu0574 (*flgE*), Atu1257 (*dgcA*), Atu1691 (*dgcB*), Atu2179 (*dgcC*), and Atu3318 (encoding a LuxR family protein). These plasmids were introduced into the wild type and the Δ*visR* mutant (in both cases the EPS$^-$UPP$^+$ background to avoid large aggregation). Measurement of β-galactosidase activity revealed expression patterns for these *lacZ* fusions that were wholly consistent with the microarray data (Fig. 6B).

DgcA, DgcB and DgcC proteins contribute to regulation of exopolysaccharides and biofilm phenotypes

Three putative *A. tumefaciens* DGC (GGDEF) proteins are implicated in the Δ*visR* phenotype: *dgcA* that was isolated from the DCR suppressor screen of the EPS$^-$UPP$^+$Δ*visR* mutant, and *dgcB* and *dgcC* that were derepressed in the *visR* mutant. To examine how these three DGC proteins might be integrated to control exopolysaccharide production in the Δ*visR* mutant, we constructed single, double and triple *dgc* deletion mutants in the Δ*visR* mutant and the otherwise wild type strain. Deletion of *dgcA* in the Δ*visR* background that also synthesizes the other polysaccharides including cellulose did not abolish elevated Congo Red Binding although this was slightly decreased relative to Δ*visR* alone (Fig. 7A). However, deletion of *dgcA* in the EPS$^-$UPP$^+$Δ*visR* background abolished its ECR phenotype (Fig. 5A). This suggests that cellulose is still up-regulated in Δ*visR*Δ*dgcA* mutants. The Δ*visR*Δ*dgcB*, Δ*visR*Δ*dgcC*, and Δ*visR*Δ*dgcB*Δ*dgcC* mutants maintained the ECR phenotype (Fig. 7A). Deletion of all three DGC genes together in Δ*visR* mutant, however, resulted in Congo Red staining marginally less intense than the Δ*visR* mutant, suggesting that DgcA and DgcB are primarily involved in stimulating cellulose and UPP production, but that DgcC may have a modest contribution.

In the Δ*visR* mutant the Δ*dgcA* mutation on its own dramatically decreased biofilm formation (Fig. 7B). The Δ*visR*Δ*dgcB*, Δ*visR*Δ*dgcC*, and Δ*visR*Δ*dgcB*Δ*dgcC* mutants maintained elevated biofilm phenotypes similar to Δ*visR* (Fig. 7B). Three way mutation of *dgcA*, *dgcB and dgcC* in the Δ*visR* mutant did not further decrease biofilm formation lower than the Δ*visR*Δ*dgcA* mutant. In the wild type, none of the DGC deletions altered its pale Congo Red staining (Fig. 7C). Deletion of either *dgcA* or *dgcB* in the otherwise wild type strain resulted in a significant biofilm reduction, whereas the Δ*dgcC* mutant forms biofilms similar to wild type (Fig. 7D). Biofilm formation of a Δ*dgcA*Δ*dgcB* double deletion mutant was completely abolished in the wild type background (Fig. 7D), suggesting that both DgcA and DgcB contribute significantly to UPP control and biofilm formation. Complementation of the Δ*dgcA* mutation or the Δ*visR*Δ*dgcA* mutation with a plasmid-borne P_{lac}-*dgcA* partially restores biofilm formation (Fig. S6A and B). A plasmid-borne P_{lac}-*dgcB* in the Δ*dgcB* mutant enhances biofilm formation roughly 3 times above wild type levels (Fig. S6A). Individual deletion of *dgcA*, *dgcB* and *dgcC* did not impact swimming motility nor did ectopic expression of these DGC genes (Fig. S6C).

Plasmid borne *lacZ* fusions of the *dgcA*, *dgcB* and *dgcC* upstream regions were used to evaluate expression in the static culture conditions of the biofilm assays. All three fusions imparted significant, detectable β-galactosidase activity to otherwise wild type *A. tumefaciens* (Fig. S6D). Interestingly, the *dgcB-lacZ* fusion has the weakest relative expression while it manifests the most profound biofilm defect (Fig. 7D).

Catalytic site mutation of DGC genes

In order to test whether the *dgcA*, *dgcB* and *dgcC* genes require their GGEEF presumptive catalytic sites (Fig. S1B) to stimulate target phenotypes and drive c-di-GMP synthesis we created plasmid-borne mutant alleles in which the GGEEF motifs were modified to GGAAF. We introduced these plasmids and their wild type counterparts into *A. tumefaciens* C58. Both the P_{lac}-*dgcA* and P_{lac}-*dgcB* plasmids with the unaltered GGEEF motif conferred the ECR phenotype on solid medium with Congo Red (Fig. 8A). While the P_{lac}-*dgcA* plasmid modestly enhanced the biofilm formation of the wild type strain, the P_{lac}-*dgcB* plasmid significantly enhanced biofilm formation similarly to when P_{lac}-*pleD* was expressed ectopically (Fig. 8B). Both of their GGAAF mutant derivatives were greatly diminished for these effects (Fig. 8A and B). In contrast, the P_{lac}-*dgcC* had no effect in a wild background and not surprisingly, this was similar for the GGAAF mutant allele (Fig. 8A and B). Direct measurement of c-di-GMP levels for *A. tumefaciens* harboring these plasmids agreed with these phenotypic patterns, with the *dgcA* and *dgcB* plasmids driving significant increases in signal concentration, whereas their GGAAF mutants did not (Fig. 8C). Again, neither the wild type nor the GGAAF form of the P_{lac}-*dgcC* plasmid significantly elevated c-di-GMP levels in *A. tumefaciens*. These same plasmids were introduced into *E. coli* DH5α and cytoplasmic c-di-GMP levels were measured (Fig. 8D). The P_{lac}-*dgcA* and P_{lac}-*dgcB* plasmids stimulated c-di-GMP levels significantly above the plasmid-free background, whereas these levels in their mutant derivatives with GGAAF mutations were severely decreased. Similar to the observations in *A. tumefaciens,* neither of the P_{lac}-*dgcC* plasmids significantly altered the c-di-GMP concentrations (Fig. 8D). These observations provide evidence that DgcA and DgcB are active DGC enzymes and their effect on exopolysaccharide synthesis and biofilm formation is mediated through their ability to catalyze c-di-GMP synthesis. Thus far we have yet to identify conditions under which DgcC is enzymatically active.

Average intracellular c-di-GMP levels do not change in visR or DGC mutants

In many ways, the Δ*visR* mutant appeared to mimic the phenotypes of strains ectopically expressing *pleD*. In addition, ectopically expressing *dgcA* or *dgcB* in an otherwise wild type

strain also resulted in the ECR phenotype, increased attachment and elevated c-di-GMP. All of these effects were dependent on the GGEEF motifs. In light of our findings that these DGCs contribute to the ECR and biofilm phenotype of *visR* mutant, we hypothesized that similar to ectopic *pleD* expression, the Δ*visR* mutant might lead to elevation of c-di-GMP. Analysis of extracts from the Δ*visR* mutant in fact revealed intracellular c-di-GMP levels that were statistically indistinguishable from the parent strain (Fig. 7E). Furthermore, mutation of *dgcA*, *dgcB* or *dgcC* in the wild type or the Δ*visR* mutants did not reveal any statistically significant decreases in c-di-GMP pools (Fig. 7E). This was also true for a Δ*visR*Δ*dgcA*Δ*dgcB*Δ*dgcC* quadruple mutant (Fig. 7E).

Mutation of a specific dual GGDEF-EAL protein causes dysregulation of UPP synthesis

The important role of c-di-GMP in controlling attachment in *A. tumefaciens* is now clear, at least in part via the VisNR regulation of DgcA and DgcB, and through them, cellulose and UPP. In many bacterial systems, production of c-di-GMP by DGC activity is balanced by degradation of the signal by PDE enzymes. In fact, the last class of *A. tumefaciens* mutants identified in the original ECR screen (Class ECR4) implicates such a PDE activity. Six independent transposon insertions were isolated in the gene cluster Atu3495–3497 (Fig. 9A). Atu3495 is the last gene in this cluster and encodes a presumptive dual function PDE protein with distinct cytoplasmic GGDEF and EAL domains, and two predicted N-terminal transmembrane segments flanking a periplasmic loop (Fig. S1). Atu3496 and Atu3497 are conserved hypothetical proteins. It seemed likely that the transposon insertions in Atu3496 and Atu3497 were polar on the downstream Atu3495. Targeted deletion of Atu3495 in the $EPS^{-}UPP^{+}$ parent resulted in the same ECR phenotype as the transposon mutants (Fig. 9B), and this mutant produced a high frequency of fl-WGA-labeled UPP in colonies (Fig. 9C). Similarly, deletion of Atu3495 in a wild type background results in the ECR phenotype and increased biofilm formation (Fig. 9D and E). The mutant is effectively complemented by introduction of a plasmid-borne P_{lac}-Atu3495 (Fig. 9D and E). The Atu3495 mutant phenotype simulates elevated PleD activity and it seems plausible that this may result from loss of its PDE function, thus leading to increased c-di-GMP.

Discussion

During surface colonization, motile bacteria must transition from an active swimming mode to an attached sessile existence. A significant component of this transition is a change in synthesis of surface polysaccharides (Branda et al., 2005). Consistent with our prior work (Xu et al., 2012), we provide evidence here that production of UPP is required for productive surface interactions in the wild type and in hyper-biofilm forming mutants. Cellulose can contribute to increased biofilm formation, particularly in strains that over produce it, but under laboratory conditions mutants unable to synthesize cellulose adhere to abiotic surfaces equivalently to the wild type. Our findings are consistent with the general observation that c-di-GMP regulates polysaccharide synthesis (Ryan et al., 2006), with elevated levels of the signal through the activity DGC genes (such as *pleD*, *dgcA* or *dgcB*) stimulating cellulose and UPP synthesis, and thus promoting attachment and subsequent biofilm formation. The activities of DGC and PDE enzymes are required to control these processes, but do not necessarily alter overall c-di-GMP levels in *A. tumefaciens.*

Regulation of surface-dependent UPP production and attachment

Initial surface association often begins with a reversible binding step, mediated by flagella and pili (O'Toole & Kolter, 1998, Merritt et al., 2007), followed by a more permanent attachment that coincides with production of one or more exopolysaccharides (Xu et al., 2012, Berk *et al.*, 2012, Colvin *et al.*, 2012). For *Caulobacter crescentus*, reversible surface contact stimulates the just-in-time production of the holdfast adhesive, produced at the tip of

this bacterium's stalk (Li et al., 2012). Similarly, production of the UPP polar adhesin in *A. tumefaciens* is also dependent on surface contact. Time-lapse total internal reflectance fluorescence (TIRF) microscopy with fluorescently tagged lectin revealed that *A. tumefaciens* deploys the UPP very rapidly, as early as several minutes upon surface binding (Li et al., 2012). Although few if any isolated planktonic *A. tumefaciens* cells produce UPP, a majority of them elaborate UPP after they bind to surfaces, either biotic (other cells, plant roots, etc) or abiotic. *A. tumefaciens* is apparently recognizing the consequences of intimate surface contact and as with *C. crescentus*, responding by transitioning to the stably adherent state.

How might *A. tumefaciens* sense solid surfaces to drive irreversible attachment and proceed forward to biofilm formation? In *C. crescentus* production of the holdfast can be stimulated by the addition of chemical agents that cause polymer crowding and impede the rotation of the flagellum (Li et al., 2012). Arguably the best-studied system is *Vibrio parahaemolyticus* in which surface contact is sensed via impeded rotation of a single polar flagellum, which activates production of a lateral flagellar (Laf) system that mediates the transition from swimming to swarming (McCarter *et al.*, 1988, McCarter & Silverman, 1990). Molecular genetic analyses have identified several of the key regulators that are required to control this process in *V. parahaemolyticus*, but the mechanism by which flagellar rotation is coupled to Laf system activation has remained elusive. In *A. tumefaciens*, mutants that block flagellar assembly are not affected for the timing or production of UPP (Xu et al., in preparation). There are now many studies showing that elevated c-di-GMP promotes sessility and biofilm formation (Ryan et al., 2006), although our findings provide the first evidence that aberrantly elevated c-di-GMP decouples the control of adhesin synthesis from surface contact. We propose that during normal *A. tumefaciens* surface colonization, a consequence or attribute of surface contact stimulates an increase of c-di-GMP through DGC activity (and possibly decreased PDE activity), thus elevating adhesin production and eventually driving biofilm formation. The apparent co-regulation of UPP and cellulose by c-di-GMP also suggests synergistic roles for these exopolysaccharides during adherent growth, with UPP providing polar surface binding and cellulose bridging cells within developing biofilms or aggregates.

Inverse control of motility and attachment via VisN and VisR

We have found that *A. tumefaciens* controls production of UPP and cellulose at least in part through the VisN-VisR transcriptional regulators, previously found to activate flagellar assembly in the rhizobia (Sourjik et al., 2000). VisN and VisR thus are well positioned at the fulcrum between motility and sessility, and exert an inhibitory influence on production of both the UPP and cellulose (Fig. 10). As in *S. meliloti*, our genetic analysis suggests that VisN and VisR function together, but that each is required for regulation. Mutations in *visN* or *visR* in *A. tumefaciens* decouple UPP production from surface dependence and ectopic expression of these regulators can severely suppress UPP production, preventing surface attachment. Microarray analysis of the Δ*visR* mutant revealed the decreased expression of several exopolysaccharide synthesis genes (most involved in succinoglycan biosynthesis) in Δ*visR*, but none of the recognized UPP and cellulose biosynthesis genes were affected by the Δ*visR* mutation. As predicted by the microarray data, synthesis of the exopolysaccharide succinoglycan (SCG) is significantly decreased in the *visR* mutant and is inhibited at high levels of c-di-GMP (Xu et al., in preparation). Differences in colony muciody also reflect this pattern as *A. tumefaciens* derivatives with elevated UPP and cellulose form dry, non-mucoid colonies (for examples see Fig. 1C, S2B and others)

In *S. meliloti* VisN-VisR activate expression of the transcription factor called Rem, a two-component-type response regulator with no known cognate histidine kinase (Rotter et al., 2006). Rem is the direct activator of many of the class II and class III flagellar genes and *S.*

meliloti rem mutants are aflagellate. One of the most dramatically decreased genes in the *A. tumefaciens* Δ*visR* mutant is *rem*, consistent with a similar regulatory architecture for flagellar assembly control as in *S. meliloti*. It is plausible that the impact of *visN* and *visR* mutations on UPP and cellulose production is also indirect through their control of *rem* expression. A simple prediction of this model, would be for *rem* mutants to phenocopy *visN* and *visR* mutants, but this is not the case in *A. tumefaciens* (Fig. 10), and our preliminary findings suggest that VisN-VisR-dependent control of adhesive polysaccharides is distinct from their control of flagellar assembly through Rem (Xu et al., in preparation)

Control of UPP and cellulose through c-di-GMP and specific DGCs

Levels of c-di-GMP have a profound influence on the attachment process in *A. tumefaciens*, consistent with findings in other bacteria (Hengge, 2009). The observed dysregulated UPP production and enhanced attachment of *visNR* mutants are highly dependent on a specific diguanylate cyclase protein, DgcA. Although two other GGDEF proteins, encoded by *dgcB* and *dgcC* are shown here to be within the VisR regulon and contribute to the ECR phenotype of the Δ*visR* mutant, DgcA plays the dominant role in the *visR* mutant. However, VisR does not influence the transcription of *dgcA* and thus we presume that this control is indirect through an additional target gene(s) the product(s) of which ultimately controls DgcA post-transcriptionally or regulates a downstream effector dependent on DgcA. Interestingly, DgcB apparently plays an equally important role in the wild type, with both *dgcA* and *dgcB* required for normal UPP-dependent attachment. For most of the DGC proteins analyzed in this study, mutation of their GGEEF motifs to GGAAF resulted in a loss of function. PleD, DgcA and DgcB require this motif to drive c-di-GMP synthesis when expressed in *E. coli*, and also in *A. tumefaciens*. Correspondingly, they also require these presumptive catalytic residues to control output phenotypes such as UPP production and cellulose synthesis. This is strong evidence that these outputs are affected by c-di-GMP produced by these proteins. Despite its parallel regulation by VisR we have yet to detect DGC activity for the *dgcC* gene product. Mutations in this gene also have little if any effect on any of the output phenotypes we have measured. Its putative GGEEF motif is not notably different from *dgcA* and *dgcB* and it may be that its activity is controlled by an environmental stimulus absent in our culture conditions. There are also examples of GGDEF proteins that do not function as enzymes but are instead regulated by c-di-GMP (Sondermann *et al.*, 2012), and it is possible that *dgcC* is not an active DGC.

Given that allosteric control of polysaccharide biosynthetic machinery by c-di-GMP is well established (Merighi *et al.*, 2007, Weinhouse *et al.*, 1997, Lee *et al.*, 2007), it is plausible that the regulation of the GGDEF proteins by VisR imparts direct control on the synthesis of cellulose and UPP. The CelA protein contains a recognized PilZ-type domain, a likely binding site for c-di-GMP (Schirmer & Jenal, 2009). Our results suggest that mutants in *visR* and *visN* are elevated for cellulose via the activity of one or more of the DGCs (*dgcA*, *dgcB*, and *dgcC*) we have identified. The simplest model is that c-di-GMP synthesized by these proteins (artificially simulated when the PleD DGC is ectopically expressed), activates cellulose synthesis via interaction with the CelA PilZ domain, although more complex models are also plausible.

We hypothesize that the rapid and surface-dependent deployment of the UPP is also allosterically regulated by c-di-GMP. *A. tumefaciens* only encodes two PilZ domain-containing proteins in addition to CelA, but neither of these have an impact on UPP production (Xu and Fuqua, unpublished results). However, there are several distinct c-di-GMP response mechanisms in addition to the activity of PilZ domains, including other protein domains that bind the signal (Hickman & Harwood, 2008, Krasteva *et al.*, 2010) and a c-di-GMP-dependent riboswitch (Sudarsan *et al.*, 2008). Several of the proteins with these c-di-GMP binding domains are transcriptional regulators, and given that VisN and VisR are

LuxR-FixJ-type transcription factors, but have atypical N-terminal domains it is plausible that a presumptive VisNR heterodimer might bind to c-di-GMP. If this were the case we would predict that this interaction would inactivate VisNR, and thereby relieve a repressive effect on UPP production, as well as block activation of *rem* and biosynthesis of flagella. However, the elevated UPP phenotype of the Δ*visR* mutant requires the activity of *dgcA*, and its ability to synthesize c-di-GMP. Thus any interaction of c-di-GMP with VisNR that might exist does not explain the increased production of UPP in the *visR* mutant. Moreover, expression analysis failed to identify the elevated expression of any UPP biosynthesis genes in the Δ*visR* mutant, which seems to rule out a simple transcription control model. We suspect that analogous to cellulose synthesis, c-di-GMP regulates one or more of the rate-limiting steps of UPP synthesis through direct interactions with the biosynthetic machinery. Recent studies in *E. coli* have revealed direct c-di-GMP regulation of poly-*N*-acetyl glucosamine (PAG) synthesis by binding to a biosynthetic enzyme, promoting its productive interaction with other components of the biosynthetic machinery (Steiner *et al.*, 2012).

Integration of c-di-GMP signaling in A. tumefaciens

There are 31 gene products with putative GGDEF domains in the *A. tumefaciens* C58 genome, 16 of which also carry annotated EAL domains (Goodner *et al.*, 2001, Slater *et al.*, 2009). How those GGDEF and EAL proteins integrate together to produce coherent, discrete output signals remains unclear. Although UPP control in wild type *A. tumefaciens* appears to be mediated primarily through *dgcA* and *dgcB*, this can be overridden by ectopic expression of *pleD,* dramatically increasing cytoplasmic levels of c-di-GMP. This in turn leads to increased production of cellulose and the UPP, and consequently to increased attachment, aggregation and biofilm formation. The mutants for *visN* and *visR* recapitulate the effect of *pleD* ectopic expression, but these phenotypes are not dependent on PleD*,* and rather on DgcA. In striking contrast to cells with high levels of PleD, the c-di-GMP levels in the Δ*visR* mutant are not significantly different from wild type. Despite the clear role of *dgcA* in UPP production in the Δ*visR* mutant, only simultaneous mutation of *dgcA*, *dgcB*, and *dgcC* decreases cellulose-dependent Congo Red staining. None of the *dgc* deletion mutants are impacted for their average levels of intracellular c-di-GMP. These observations are in agreement with a number of recent studies in which the cytoplasmic levels of c-di-GMP fail to correlate with specific targeted phenotypes. In *P. aeruginosa* two DGC proteins, SadC and RoeA predominantly regulate distinct target functions (motility and polysaccharide synthesis, respectively), and in both cases control requires their catalytic GGDEF/GGEEF motif, indicating the requirement for c-di-GMP (Merritt *et al.*, 2010). However, cellular levels of c-di-GMP do not correlate with changes in the DGC-regulated phenotypes, leading to the proposal that the targets which control these phenotypes only perceive the c-di-GMP synthesized by a specific DGC enzyme(s), and that the signal is somehow compartmentalized, not contributing to the average cytoplasmic signal concentration. Likewise, studies in *E. coli* suggest that the oxygen-responsive DGC/PDE pair DosC and DosP form a complex with their target enzyme, polynucleotide phosphorylase, and control its activity through localized synthesis and degradation of c-di-GMP (Goodner et al., 2001). It is however clear that compartmentalization of c-di-GMP signaling is not the only way to achieve specificity, as in *V. cholerae* the VpsT transcription factor responds to c-di-GMP synthesized by five different DGCs and these can act on VpsT from a distance (Hengge, 2009). We did not observe global changes in the levels of c-di-GMP in the *A. tumefaciens visR* mutant, although its phenotype requires *dgcA* and its GGEEF motif. Our findings suggest that increases in c-di-GMP for this mutant may occur in a localized fashion, potentially at the cell pole where UPP is synthesized.

Experimental procedures

Reagents, strains and growth conditions

All strains, plasmids and oligonucleotides used in this study are provided in the Supplementary Materials, Tables S3 and S4, respectively. The *E. coli* strains used for plasmid DNA transformation or conjugation of plasmids were grown in LB broth (Difco Bacto tryptone at 10 g liter^{-1}, Difco yeast extract at 10 g liter^{-1}, and NaCl at 5 g liter^{-1}, pH 7.2) with or without 1.5% (w v^{-1}) agar. Unless noted otherwise, the *A. tumefaciens* strains were grown on either LB or AT minimal medium (Tempe *et al.*, 1977) supplemented with 0.5% (wt vol^{-1}) glucose and 15 mM ammonium sulfate (ATGN). To prevent the accumulation of iron oxide precipitate, the $FeSO_4$ prescribed in the original AT recipe was omitted, with no adverse growth effect. However, for biofilm cultures, 22 μM $FeSO_4{\cdot}7H_2O$ was added to ATGN medium immediately before. For *sacB* counter-selection, 5% sucrose (Suc) replaced glucose as the sole carbon source (ATSN). Chemicals, antibiotics, and culture media were obtained from Fisher Scientific and Sigma-Aldrich. When required, appropriate antibiotics were added to the medium as follows: for *E. coli*, 50 μg ml^{-1} ampicillin, 25 μg ml^{-1} gentamicin (Gm), 50 μg ml^{-1} kanamycin (Km) and 100 μg ml^{-1} spectinomycin; and for *A. tumefaciens*, 300 μg ml^{-1} gentamicin, 150 μg ml^{-1} Km, and 200 μg ml^{-1} spectinomycin. Isopropyl-β-D-thiogalactopyranoside (IPTG) was used when necessary. For Congo Red plates, the dye was dissolved in methanol at 20 mg/ml, and passed through 0.2 μm syringe filters immediately before use to remove aggregates. Four ml filtered Congo Red was added per L (final ~80 μg/ml) to generate ATGN-CR agar medium.

Transposon mutagenesis

The *mariner* minitransposon *Himar1* was used to mutagenize *A. tumefaciens* C58 (Lampe *et al.*, 1999). Fully turbid LB-broth cultures of the donor *E. coli* SM10/λ*pir* pFD1 (*Himar1*) and *A. tumefaciens*, were inoculated at a 1:10 dilution in 2 mls of LB broth and incubated 4 h at 37°C and 27°C respectively. From each culture 1 ml was removed and cells were collected by centrifugation (6,000 × g) and resuspended in 50 μl of LB. From each cell suspension 50 μl were mixed together and this entire mixture was spotted on 0.2 μm cellulose acetate filters on a LB plate without antibiotics. After the inoculant soaked in, these plates were incubated overnight at 28°C to allow mating. Following incubation, cells were suspended off the filter into 1 ml sterile 30% glycerol, and then, aliquots serially diluted (10^{-1}–10^{-5}) with 100 μl plated on Congo Red ATGN media with appropriate levels of Km, followed by incubation at 28°C. The unused mating mixture was frozen at −80°C for subsequent platings, as necessary.

Touchdown PCR and sequencing

Genomic DNA was isolated from Mariner mutagenized *A. tumefaciens* derivatives using a Wizard Genomic DNA purification kit (Promega Corp.). The genomic DNA concentration was measured using a NanoDrop 1000 Spectrophotometer (Thermo Scientific). Touchdown PCR was performed using 80–120 ng genomic DNA with primers MarRSeq and MarTDL2 pair or MarLSeq and MarTDR1 pair (Table S4), and NEB High Fidelity Phusion polymerase, followed with a standard Touchdown PCR program [(i) 54 min, 95 °C, (ii) 24 cycles, 95 °C for 45 sec, 60 °C for 45 sec decreasing by 5 degrees with each cycle, 2 min at 72 °C, and (iii) 24 cycles, 95 °C for 45 sec, 60 °C for 45 sec, 2 min at 72 °C]. PCR reactions that yielded one or several strong bands were purified using Qiagen Qiaquick purification kit and used as template for cycle sequencing using the Big Dye reagent, primers MarRSeq or MarLseq and the recommended protocol in the Indiana Molecular Biology Institute.

UPP production assays

The UPP was visualized as described using wheat germ agglutinnin (WGA) labeled with Alex Fluor 594 (Invitrogen). *A. tumefaciens* were grown in ATGN to an optical density of approximately 0.6 at 600 nm (OD_{600}). A 1 ml aliquot of culture was centrifuged (6,000 × g) and pelleted cells were resuspended in 100 ATGN. To visualize the production of UPP in standard colonies on agar, these were picked with a sterile toothpick and suspended in 100 μl ATGN. In both cases, 1μl labeled WGA stock solution (1 mg ml^{-1}) was added to 100 μl of the suspension and incubated for 20 min. Bacteria were collected by centrifugation (6,000 × g) and washed twice by ATGN medium. A small volume of the cell suspension was dispensed on an agar pad (1.5 % agar, 150 μl) solidified on a microscopic slide, just prior to application of a coverslip. Samples were observed by fluorescence microscopy (Nikon E800) using a 100× oil immersion objective and NIS-Elements software.

Cultivation and analysis of static culture biofilms

Biofilms were grown in static culture essentially as described previously (Merritt et al., 2007). Briefly, sterile polyvinyl chloride (PVC) coverslips were placed vertically in 12-well polystyrene cell culture plates (Corning Inc.), inoculated with cells in ATGN at an OD600 of 0.05, and incubated at room temperature for 48 h. For CV visualization, coverslips were rinsed in double-distilled H_2O, stained with 0.1% (wt vol^{-1}) CV for 10 min, and rinsed again in double-distilled H_2O. CV-stained biomass adhered to the coverslip was quantified by soaking stained coverslips in 1 ml of 33% acetic acid to solubilize the CV, followed by absorbance measurement of the soluble stain at 600 nm (A_{600}) in a Bio-Tek Synergy HT microplate reader. Absorbance values were normalized to culture growth by dividing the A_{600} value for solubilized CV by the OD_{600} value of the planktonic culture.

Expression analysis using DNA microarrays

A. tumefaciens C58 specific microarrays created with custom 60mer oligonucleotides were purchased from Agilent Technologies. RNA was extracted with the RNeasy Kit (Qiagen) as per the manufacturer's instructions. Transcriptional profiling was carried out as follows with 20 mg of purified RNA used for cDNA synthesis. First strand labeling and reverse transcription was performed using Invitrogen SuperScript Indirect Labeling Kit, and cDNA was purified on Qiagen QIAQuick columns. cDNA was labeled with AlexaFluor 542 and 655 dyes using Invitrogen SuperScript cDNA Labeling Kit, and repurified on QIAQuick columns. The yield and purity of cDNA was quantified on a NanoDrop spectrophotometer. Hybridization reactions were performed using an Agilent *in situ* Hybridization Kit Plus. Equivalent amounts of labeled cDNA preparations were mixed 50/50, boiled for 5 min at 95°C, applied to the *A. tumefaciens* C58 custom microarrays, and hybridized overnight at 65°C. Hybridized arrays were washed with Agilent Wash Solutions 1 and 2, rinsed with acetonitrile, and incubated in Agilent Stabilization and Drying Solution immediately prior to scanning the arrays. Four independent biological replicates were performed for comparison of the wild type and the Δ*visR* mutant, with dye swaps. Hybridized arrays were scanned on a GenePix Scanner 4200. Scanned images were processed by the LIMMA package in Bioconductor, correcting for background with the minimum method, normalizing within arrays with the LOESS method, and between arrays with the quantile method. Linear model fitting and empirical Bayesian analysis was performed by least squares, and dye swap effect correction. Gene lists were created using a *t*-test P-value < 0.05 and with $\log_2$ ratios of ≥ 0.6 or ≤ −0.6 (representing a fold-change of ± 1.5) are reported here. Microarray data is deposited into the Gene Expression Omnibus (GEO) database (http://www.ncbi.nlm.nih.gov/geo/)

Electron microscopy

Electron microscopy was performed in the Indiana Molecular Biology Institute Microscopy Center. For scanning electron microscopy (SEM), 10 ul 1% poly L-lysine was added to the surface of a disk-shaped glass coverslip for 5 min to make the surface adhesive. The coverslip was rinsed with water, and 10 μl of culture (OD_{600} 0.6) was added to the coverslip surface for 5 min and absorbed by filter paper. Bacteria remaining on the coverslip were fixed with 10 μl 2% glutaraldehyde in 0.2 M sodium cacodylate buffer (pH 7.2) for 5 min. Bacteria on coverslips were dried by treatment with a series of increasing ethanol solutions (30%–100%). These coverslips were further dried in an atmosphere saturated with absolute ethanol and then dehydrated with acetone and dried with CO_2 using the critical point method. The samples were sputter coated with gold and observed by a JEOL JSM-5800 LV Scanning Electron Microscope at 10 kV.

For Immuno-gold Transmission Electron Microscopy (TEM), 1 ml of culture (OD_{600} 0.6) was centrifuged and resuspended in 200 μl ATGN, to which 5 μl 20 nm colloidal gold conjugated WGA (20 μg/ml WGA, purchased from EY laboratories) was added and incubated 20 min. The bacterial suspension was centrifuged (6,000 × g) and the pelleted material was washed twice with 1 ml ATGN and resuspended in 200 μl ATGN. 10 μl of bacterial suspension was applied to carbon-coated grids for 5 min and stained with 10 μl 1% uranyl acetate 5 min. Excess uranyl acetate was removed using filter paper and the grid was air dried for 5 min. The grid was then examined using the JEOL JEM-1010 Transmission Electron Microscope at 80 kV.

Motility assays and flagellar staining

Motility plates were performed using 100-mm petri plates with 25 ml ATGN medium containing 0.3% Bacto agar (BD). Motility plates were inoculated with 5 μl of fresh cultures (OD_{600}=0.6) at the center of the plate, plates were incubated for up to six days at room temperature, and the swim ring diameter was measured daily.

Flagella were stained using a two-component stain and protocol adapted from Mayfield and Inniss (Mayfield & Inniss, 1977). Solution A is equal volumes 5% phenol and saturated $AlK(SO_4)_2$ $12H_2O$ in 10% tannic acid, and solution B is 12% crystal violet (CV) in 100% ethanol. Solutions A and B were mixed fresh with 10 volumes of A added to 1 volume of B, vortexed, and centrifuged to remove CV crystals. A small volume of bacterial culture (~3 μl) was spotted onto a clean microscope slide and overlaid with a 22 × 22-mm coverslip. The slides were held vertically, and approximately 2 to 5 μl of the AB stain solution was applied to the edge of the coverslip, allowing capillary action to wick the stain under the coverslip. Samples were observed by phase-contrast microscopy using a 100× oil immersion objective after at least 5 min of staining.

c-di-GMP measurement

Cultures of *A. tumefaciens* derivatives were grown in ATGN medium (plus 0.5 mM IPTG if needed) at 28°C to OD_{600} of 2.0, and used to perform viable counts to determine CFUs/ml. Cultures of *E. coli* DH5α derivatives were grown in LB (plus 0.5 mM IPTG if needed) at 37°C to OD_{600} of 0.6–0.8. 30 ml of culture was centrifuged for 3 min at 10,000 × g at 25°C. The pellet was immediately resuspended in 250 μl extraction buffer (methanol/mcetonitrile/ dH_2O 40:40:20 + 0.1 N formic acid cooled at −20°C) by vigorous vortexing and pipetting. The extractions were incubated at −20°C for 30 min, followed by transfer to a new microfuge tube on ice. Cell debris was removed by centrifugation at 10,000 × g 5 min at 4°C, and 200 μl of supernatant was transferred into a new tube on ice. Samples were neutralized within 1 hr of preparation by adding 4 μl of 15% NH_4HCO_3 per 100 μl of sample, aimed to set a pH of 7 ~ 7.5.

Prior to analysis, the sample was subjected to vacuum centrifugation to remove the extraction buffer and resuspended in an equal volume of water. Ten μL of each sample was then analyzed using liquid chromatography coupled with tandem mass spectrometry (LC-MS/MS) on a Quattro Premier XE mass spectrometer (Waters Corporation) coupled with an Acquity Ultra Performance LC system (Waters Corporation). C-di-GMP detection and quantification was performed as previously described (Massie *et al.*, 2012). To calculate the c-di-GMP concentration, chemically synthesized c-di-GMP (Biolog) was dissolved in water at concentrations of 250, 125, 62.5, 31.2, 15.6, 7.8, 3.9, and 1.9 nM and analyzed using LC-MS/MS to generate a standard curve.

Construction of in-frame markerless deletions

Construction of nonpolar deletion was performed as reported previously (Merritt et al., 2007). Briefly, PCR was used to amplify approximately 500 to 1,000 bp of flanking sequence upstream (primers 1 and 2) and downstream (primers 3 and 4) of the reading frame targeted for deletion. Primers were designed to remove as much of the coding sequence as possible without disrupting any possible translational coupling. Primers 2 and 3 were designed with 18-bp complementary sequences at their 5′ ends (lowercase nucleotides in Table S4) to facilitate *s*plicing by *o*verlapping *e*xtension (SOE), essentially as described previously (Merritt et al., 2007). Briefly, both flanking sequences were amplified using the high-fidelity Phusion DNA polymerase (NEB) and were agarose gel purified. Purified PCR products were used as both templates and primers for a five-cycle PCR. A final PCR step with primers 1 and 4, using 2 μl of the second-step reaction mix as the template, generating the full-length spliced product. The final PCR products were cloned into pGEM-T Easy (Promega), confirmed by sequencing, excised by cleavage with the appropriate restriction enzymes, and ligated with the suicide vector pNPTS138 cleaved at compatible restriction sites. The pNPTS138 plasmid confers Km resistance (Km^R) and sucrose sensitivity (Suc^s). Derivatives of pNPTS138 were introduced into *A. tumefaciens* C58 by electroporation. The ColE1 origin of pNPTS138 does not replicate in *A. tumefaciens*, and therefore the plasmid must recombine into the genome, to allow growth of transformants on media containing Km. Recombinants were selected on ATGN plates containing Km^R, and plasmid integration was confirmed by patching Km^R isolates onto ATSN-Km plates to identify Suc^S derivatives. To facilitate excision of the integrated plasmid, Km^R Suc^S clones were grown overnight in ATGN broth without Km^R and then plated on ATSN. Plasmid excision was verified by patching Suc^Rclones onto ATSN plus Km to identify Km^S derivatives. Appropriate deletion of the target genes was confirmed by diagnostic PCR and DNA sequencing of the products.

Controlled expression plasmids

To perform complementation analyses, wild-type coding sequences were cloned into the $LacI^Q$ encoding, IPTG-inducible expression vector pSRKKm or pSRKGm (Khan *et al.*, 2008). Coding sequences were PCR amplified from C58 genomic DNA, using the corresponding primers for each gene (Table S4) and the Phusion polymerase. Amplicons were ligated into pGEM-T Easy, confirmed by sequencing, excised by restriction enzyme cleavage, and ligated with appropriately cleaved pSRKKm or pSRKGm. Plasmid derivatives harboring the correct inserts were verified by restriction digestion and sequencing prior to electroporation into competent *A. tumefaciens* cells.

Catalytic site mutations for PleD, DgcA, DgcB and DgcC

These site-specific mutants were generated by PCR SOEing with mutagenic primers. Mutagenesis of *pleD* is an example. Complementary primers pairs (*pleD**-P1 and *pleD**-P2) were designed with GGEEF mutated to GGAAF by altering the corresponding nucleotides in the internal primers. The first round of PCR reactions were performed by using primer pairs (Com-*pleD*-P1 and *pleD**-P2) and (Com-*pleD*-P2 and *pleD**-P1) separately to amplify

the sequences from C58 genomic DNA. Amplicons from the previous two PCR reactions were gel purified and added as the template for the second round of PCR by using Com-*pleD*-P1 and Com-*pleD*-P2. The amplicons from the second round of PCR were gel purified, excised by restriction enzyme cleavage and ligated with appropriately cleaved pSRKGm. Plasmid derivatives harboring the correct inserts were verified by restriction digestion and sequencing prior to electroporation into competent *A. tumefaciens* cells. Catalytic site mutations for DgcA, DgcB and DgcC were constructed by the same approach.

β-Galactosidase assays and lacZ fusions

Fragments containing the promoter elements upstream of Atu1257, Atu1691, Atu2179, Atu3318, Atu0560, Atu0573 and Atu0574 were amplified from *A. tumefaciens* genomic DNA using Phusion DNA polymerase and primers 1 and 2 (see Table S4). PCR fragments were agarose gel purified, ligated into pGEM-T Easy, and verified by sequencing. Fragments were excised with the appropriate restriction enzymes and ligated into the compatibly cleaved vector pRA301. Fragments were designed to insert the promoter region and ribosome binding site with the start codon of the gene of interest in frame with the promoterless *lacZ* gene. Fragments were confirmed by PCR, and the constructs were electroporated into *A. tumefaciens* wild-type and mutant derivatives.

Cultures were prepared for β-galactosidase assay by culturing in ATGN into exponential phase measured for OD_{600} and frozen at −80°C. The β-galactosidase activity of the cultures was assayed as described previously (Hibbing & Fuqua, 2011). Briefly, cells were permeabilized in Z-buffer (0.06 M Na_2HPO_4, 0.04 M NaH_2PO_4, 0.01 M KCl, 0.001 M $MgSO_4$, 0.05 M β-mercaptoethanol, pH 7.0) by the addition of 3 drops of 0.05% SDS and 4 drops of chloroform. β-galactosidase reactions were initiated by addition of 100 μl of a 4 mg ml-1 solution of the colorimetric substrate *o*-nitrophenyl β-D-galactopyranoside (ONPG) and terminated with addition of 600 μl of 6 M $NaCO_2$. Intact cells and debris were removed by centrifugation (10 min, 10,000 × g) and free ONP was measured as A_{420} and specific activity was reported in Miller Units. At least 3 biological replicates were performed.

Supplementary Material

Refer to Web version on PubMed Central for supplementary material.

Acknowledgments

This project was supported by National Institutes of Health (NIH) grants GM080546 (C.F.) and Region V ‘Great Lakes’ RCE (NIH award 2-U54-AI-057153) (C.M.W.), and through a grant from the Indiana University METACyt program, funded in part by a major endowment from the Lilly Foundation (C.F.). We thank the laboratory of Y.V. Brun and D.B. Kearns for helpful input and suggestions. We also acknowledge assistance from the IUB Light Microscopy Imaging Center, the IUB Center for Genomics and Bioinformatics and the MSU Mass Spectrometry Facility.

References

Abel S, Chien P, Wassmann P, Schirmer T, Kaever V, Laub MT, Baker TA, Jenal U. Regulatory cohesion of cell cycle and cell differentiation through Inter linked phosphorylation and second messenger networks. Mol Cell. 2011; 43:550–560. [PubMed: 21855795]

Aldridge P, Paul R, Goymer P, Rainey P, Jenal U. Role of the GGDEF regulator PleD in polar development of *Caulobacter crescentus*. Mol Microbiol. 2003; 47:1695–1708. [PubMed: 12622822]

Amikam D, Benziman M. Cyclic diguanylic acid and cellulose synthesis in *Agrobacterium tumefaciens*. J Bacteriol. 1989; 171:6649–6675. [PubMed: 2556370]

Berk V, Fong JC, Dempsey GT, Develioglu ON, Zhuang X, Liphardt J, Yildiz FH, Chu S. Molecular architecture and assembly principles of *Vibrio cholerae* biofilms. Science. 2012; 337:236–239. [PubMed: 22798614]

Blair KM, Turner L, Winkelman JT, Berg HC, Kearns DB. A molecular clutch disables flagella in the *Bacillus subtilis* biofilm. Science. 2008; 320:1636–1638. [PubMed: 18566286]

Branda SS, Vik S, Friedman L, Kolter R. Biofilms: the matrix revisited. Trends Microbiol. 2005; 13:20–26. [PubMed: 15639628]

Brown PJ, de Pedro MA, Kysela DT, Van der Henst C, Kim J, De Bolle X, Fuqua C, Brun YV. Polar growth in the Alphaproteobacterial order Rhizobiales. Proc Natl Acad Sci U S A. 2012; 109:1697–1701. [PubMed: 22307633]

Brown PJ, Hardy GG, Trimble MJ, Brun YV. Complex regulatory pathways coordinate cell-cycle progression and development in *Caulobacter crescentus*. Adv Microb Physiol. 2009; 54:1–101. [PubMed: 18929067]

Cangelosi GA, Martinetti G, Leigh JA, Lee CC, Thienes C, Nester EW. Role for *Agrobacterium tumefaciens* ChvA protein in export of beta-1,2-glucan. J Bacteriol. 1989; 171:1609–1615. [PubMed: 2921245]

Cangelosi GA, Martinetti G, Nester EW. Osmosensitivity phenotypes of *Agrobacterium tumefaciens* mutants that lack periplasmic beta-1,2-glucan. J Bacteriol. 1990; 172:2172–2174. [PubMed: 2318812]

Cogan NG, Keener JP. The role of the biofilm matrix in structural development. Mathematical Medicine And Biology-A Journal Of The Ima. 2004; 21:147–166. [PubMed: 15228104]

Colvin KM, Irie Y, Tart CS, Urbano R, Whitney JC, Ryder C, Howell PL, Wozniak DJ, Parsek MR. The Pel and Psl polysaccharides provide *Pseudomonas aeruginosa* structural redundancy within the biofilm matrix. Environ Microbiol. 2012; 14:1913–1928. [PubMed: 22176658]

D'Argenio DA, Miller SI. Cyclic di-GMP as a bacterial second messenger. Microbiology. 2004; 150:2497–2502. [PubMed: 15289546]

Danhorn T, Fuqua C. Biofilm formation by plant-associated bacteria. Annu Rev Microbiol. 2007; 61:401–422. [PubMed: 17506679]

Douglas CJ, Halperin W, Nester EW. *Agrobacterium tumefaciens* mutants affected for attachment to plant cells. J Bacteriol. 1982; 152:1265–1275. [PubMed: 6292165]

Duerig A, Abel S, Folcher M, Nicollier M, Schwede T, Amiot N, Giese B, Jenal U. Second messenger-mediated spatiotemporal control of protein degradation regulates bacterial cell cycle progression. Genes Dev. 2009; 23:93–104. [PubMed: 19136627]

Goodner B, Hinkle G, Gattung S, Miller N, Blanchard M, Qurollo B, Goldman BS, Cao Y, Askenazi M, Halling C, Mullin L, Houmiel K, Gordon J, Vaudin M, Iartchouk O, Epp A, Liu F, Wollam C, Allinger M, Doughty D, Scott C, Lappas C, Markelz B, Flanagan C, Crowell C, Gurson J, Lomo C, Sear C, Strub G, Cielo C, Slater S. Genome sequence of the plant pathogen and biotechnology agent *Agrobacterium tumefaciens* C58. Science. 2001; 294:2323–2328. [PubMed: 11743194]

Hall-Stoodley L, Costerton JW, Stoodley P. Bacterial biofilms: from the natural environment to infectious diseases. Nat Rev Microbiol. 2004; 2:95–108. [PubMed: 15040259]

Hengge R. Principles of c-di-GMP signalling in bacteria. Nat Rev Microbiol. 2009; 7:263–273. [PubMed: 19287449]

Hibbing ME, Fuqua C. Antiparallel and interlinked control of cellular iron levels by the Irr and RirA regulators of *Agrobacterium tumefaciens*. J Bacteriol. 2011; 193:3461–3472. [PubMed: 21602352]

Hickman JW, Harwood CS. Identification of FleQ from *Pseudomonas aeruginosa* as a c-di-GMP-responsive transcription factor. Mol Microbiol. 2008; 69:376–389. [PubMed: 18485075]

Howie AJ, Brewer DB. Optical properties of amyloid stained by Congo red: history and mechanisms. Micron. 2009; 40:285–301. [PubMed: 19019688]

Khan SR, Gaines J, Roop RM 2nd, Farrand SK. Broad-host-range expression vectors with tightly regulated promoters and their use to examine the influence of TraR and TraM expression on Ti plasmid quorum sensing. Appl Environ Microbiol. 2008; 74:5053–5062. [PubMed: 18606801]

Kim J, Heindl JE, Fuqua C. Coordination of division and development influences complex multicellular behavior in *Agrobacterium tumefaciens*. PLOS ONE. 2013; 10:1371.

Kolter R, Greenberg EP. Microbial sciences: the superficial life of microbes. Nature. 2006; 441:300–302. [PubMed: 16710410]

Krasteva PV, Fong JC, Shikuma NJ, Beyhan S, Navarro MV, Yildiz FH, Sondermann H. *Vibrio cholerae* VpsT regulates matrix production and motility by directly sensing cyclic di-GMP. Science. 2010; 327:866–868. [PubMed: 20150502]

Lampe DJ, Akerley BJ, Rubin EJ, Mekalanos JJ, Robertson HM. Hyperactive transposase mutants of the *Himar1* mariner transposon. Proc Natl Acad Sci USA. 1999; 96:11428–11433. [PubMed: 10500193]

Lee VT, Matewish JM, Kessler JL, Hyodo M, Hayakawa Y, Lory S. A cyclic-di-GMP receptor required for bacterial exopolysaccharide production. Mol Microbiol. 2007; 65:1474–1484. [PubMed: 17824927]

Li G, Brown PJ, Tang JX, Xu J, Quardokus EM, Fuqua C, Brun YV. Surface contact stimulates the just-in-time deployment of bacterial adhesins. Mol Microbiol. 2012; 83:41–51. [PubMed: 22053824]

Mah TF, Pitts B, Pellock B, Walker GC, Stewart PS, O'Toole GA. A genetic basis for *Pseudomonas aeruginosa* biofilm antibiotic resistance. Nature. 2003; 426:306–310. [PubMed: 14628055]

Massie JP, Reynolds EL, Koestler BJ, Cong JP, Agostoni M, Waters CM. Quantification of high-specificity cyclic diguanylate signaling. Proc Natl Acad Sci U S A. 2012; 109:12746–12751. [PubMed: 22802636]

Matthysse, AG. Initial interactions of *Agrobacterium tumefaciens* with plant host cells. In: O'Leary, WM., editor. CRC Critical Reviews in Microbiology. Boca Raton: CRC Press Inc; 1986. p. 281-307.

Matthysse AG, White S, Lightfoot R. Genes required for cellulose synthesis in *Agrobacterium tumefaciens*. J Bacteriol. 1995; 177:1069–1075. [PubMed: 7860585]

Mayfield CI, Inniss WE. A rapid, simple method for staining bacterial flagella. Canadian journal of microbiology. 1977; 23:1311–1313. [PubMed: 71191]

McCarter L, Hilmen M, Silverman M. Flagellar dynamometer controls swarmer cell differentiation of *V. parahaemolyticus*. Cell. 1988; 54:345–351. [PubMed: 3396074]

McCarter L, Silverman M. Surface-induced swarmer cell differentiation of *Vibrio parahaemolyticus*. Mol Microbiol. 1990; 4:1057–1062. [PubMed: 2233248]

Merighi M V, Lee T, Hyodo M, Hayakawa Y, Lory S. The second messenger bis-(3′-5′)-cyclic-GMP and its PilZ domain-containing receptor Alg44 are required for alginate biosynthesis in *Pseudomonas aeruginosa*. Mol Microbiol. 2007; 65:876–895. [PubMed: 17645452]

Merritt JH, Ha DG, Cowles KN, Lu W, Morales DK, Rabinowitz J, Gitai Z, O'Toole GA. Specific control of *Pseudomonas aeruginosa surface-associated behaviors by two c-di-GMP diguanylate cyclases*. mBio. 2010; 19:e00183-00181. [PubMed: 20978535]

Merritt PM, Danhorn T, Fuqua C. Motility and chemotaxis in *Agrobacterium tumefaciens* surface attachment and biofilm formation. J Bacteriol. 2007; 189:8005–8014. [PubMed: 17766409]

O'Connell KP, Handelsman J. *chvA* locus may be involved in export of neutral cyclic beta-1,2-linked D-glucan from *Agrobacterium tumefaciens*. Mol Plant Microbe Interact. 1989; 2:11–16. [PubMed: 2520158]

O'Toole GA, Kolter R. Flagellar and twitching motility are necessary for *Pseudomonas aeruginosa* biofilm development. Mol Microbiol. 1998; 30:295–304. [PubMed: 9791175]

Pratt LA, Kolter R. Genetic analysis of *Escherichia coli* biofilm formation: roles of flagella, motility, chemotaxis and type I pili. Mol Microbiol. 1998; 30:285–293. [PubMed: 9791174]

Romling U. Characterization of the rdar morphotype, a multicellular behaviour in Enterobacteriaceae. Cellular and molecular life sciences : CMLS. 2005; 62:1234–1246. [PubMed: 15818467]

Römling U. Molecular biology of cellulose production in bacteria. Res Microbiol. 2002; 153:205–212. [PubMed: 12066891]

Rotter C, Muhlbacher S, Salamon D, Schmitt R, Scharf B. Rem, a new transcriptional activator of motility and chemotaxis in *Sinorhizobium meliloti*. J Bacteriol. 2006; 188:6932–6942. [PubMed: 16980496]

Ryan RP, Fouhy Y, Lucey JF, Crossman LC, Spiro S, He YW, Zhang LH, Heeb S, Camara M, Williams P, Dow JM. Cell-cell signaling in *Xanthomonas campestris* involves an HD-GYP

domain protein that functions in cyclic di-GMP turnover. Proc Natl Acad Sci USA. 2006; 103:6712–6717. [PubMed: 16611728]

Schirmer T, Jenal U. Structural and mechanistic determinants of c-di-GMP signalling. Nat Rev Microbiol. 2009; 7:724–735. [PubMed: 19756011]

Simm R, Morr M, Kader A, Nimtz M, Römling U. GGDEF and EAL domains inversely regulate cyclic di-GMP levels and transition from sessility to motility. Mol Microbiol. 2004; 53:1123–1134. [PubMed: 15306016]

Slater SC, Goldman BS, Goodner B, Setubal JC, Farrand SK, Nester EW, Burr TJ, Banta L, Dickerman AW, Paulsen I, Otten L, Suen G, Welch R, Almeida NF, Arnold F, Burton OT, Du Z, Ewing A, Godsy E, Heisel S, Houmiel KL, Jhaveri J, Lu J, Miller NM, Norton S, Chen Q, Phoolcharoen W, Ohlin V, Ondrusek D, Pride N, Stricklin SL, Sun J, Wheeler C, Wilson L, Zhu H, Wood DW. Genome sequences of three *Agrobacterium* biovars help elucidate the evolution of multichromosome genomes in bacteria. J Bacteriol. 2009; 191:2501–2511. [PubMed: 19251847]

Sondermann H, Shikuma NJ, Yildiz FH. You've come a long way: c-di-GMP signaling. Curr Opin Microbiol. 2012; 15:140–146. [PubMed: 22226607]

Sourjik V, Muschler P, Scharf B, Schmitt R. VisN and VisR are global regulators of chemotaxis, flagellar, and motility genes in *Sinorhizobium (Rhizobium) meliloti*. J Bacteriol. 2000; 182:782–788. [PubMed: 10633114]

Stasinopoulos SJ, Fisher PR, Stone BA, Stanisich VA. Detection of two loci involved in (1-->3)-beta-glucan (curdlan) biosynthesis by *Agrobacterium* sp. ATCC31749, and comparative sequence analysis of the putative curdlan synthase gene. Glycobiology. 1999; 9:31–41. [PubMed: 9884404]

Steiner S, Lori C, Boehm A, Jenal U. Allosteric activation of exopolysaccharide synthesis through cyclic di-GMP-stimulated protein-protein interaction. EMBO J. 2012; 32:354–368. [PubMed: 23202856]

Sudarsan N, Lee ER, Weinberg Z, Moy RH, Kim JN, Link KH, Breaker RR. Riboswitches in eubacteria sense the second messenger cyclic di-GMP. Science. 2008; 321:411–413. [PubMed: 18635805]

Tamayo R, Pratt JT, Camilli A. Roles of cyclic diguanylate in the regulation of bacterial pathogenesis. Annu Rev Microbiol. 2007; 61:131–148. [PubMed: 17480182]

Tempe J, Petit A, Holsters M, Montagu M, Schell J. Thermosensitive step associated with transfer of the Ti plasmid during conjugation: Possible relation to transformation in crown gall. Proc Natl Acad Sci U S A. 1977; 74:2848–2849. [PubMed: 16592419]

Van Larebeke N, Engler G, Holsters M, Van den Elsacker S, Zaenen I, Schilperoort RA, Schell J. Large plasmid in *Agrobacterium tumefaciens* essential for crown gall-inducing ability. Nature. 1974; 252:169–170. [PubMed: 4419109]

Watson B, Currier TC, Gordon MP, Chilton MD, Nester EW. Plasmid required for virulence of *Agrobacterium tumefaciens*. J Bacteriol. 1975; 123:255–264. [PubMed: 1141196]

Weinhouse H, Sapir S, Amikam D, Shilo Y, Volman G, Ohana P, Benziman M. c-di-GMP-binding protein, a new factor regulating cellulose synthesis in *Acetobacter xylinum*. FEBS Lett. 1997; 416:207–211. [PubMed: 9369216]

Wu CF, Lin JS, Shaw GC, Lai EM. Acid-induced type VI secretion system is regulated by ExoR-ChvG/ChvI signaling cascade in *Agrobacterium tumefaciens*. PLoS Pathog. 2012; 8:e1002938. [PubMed: 23028331]

Xu J, Kim J, Danhorn T, Merritt PM, Fuqua C. Phosphorus limitation increases attachment in *Agrobacterium tumefaciens* and reveals a conditional functional redundancy in adhesin biosynthesis. Res Microbiol. 2012; 163:674–684. [PubMed: 23103488]

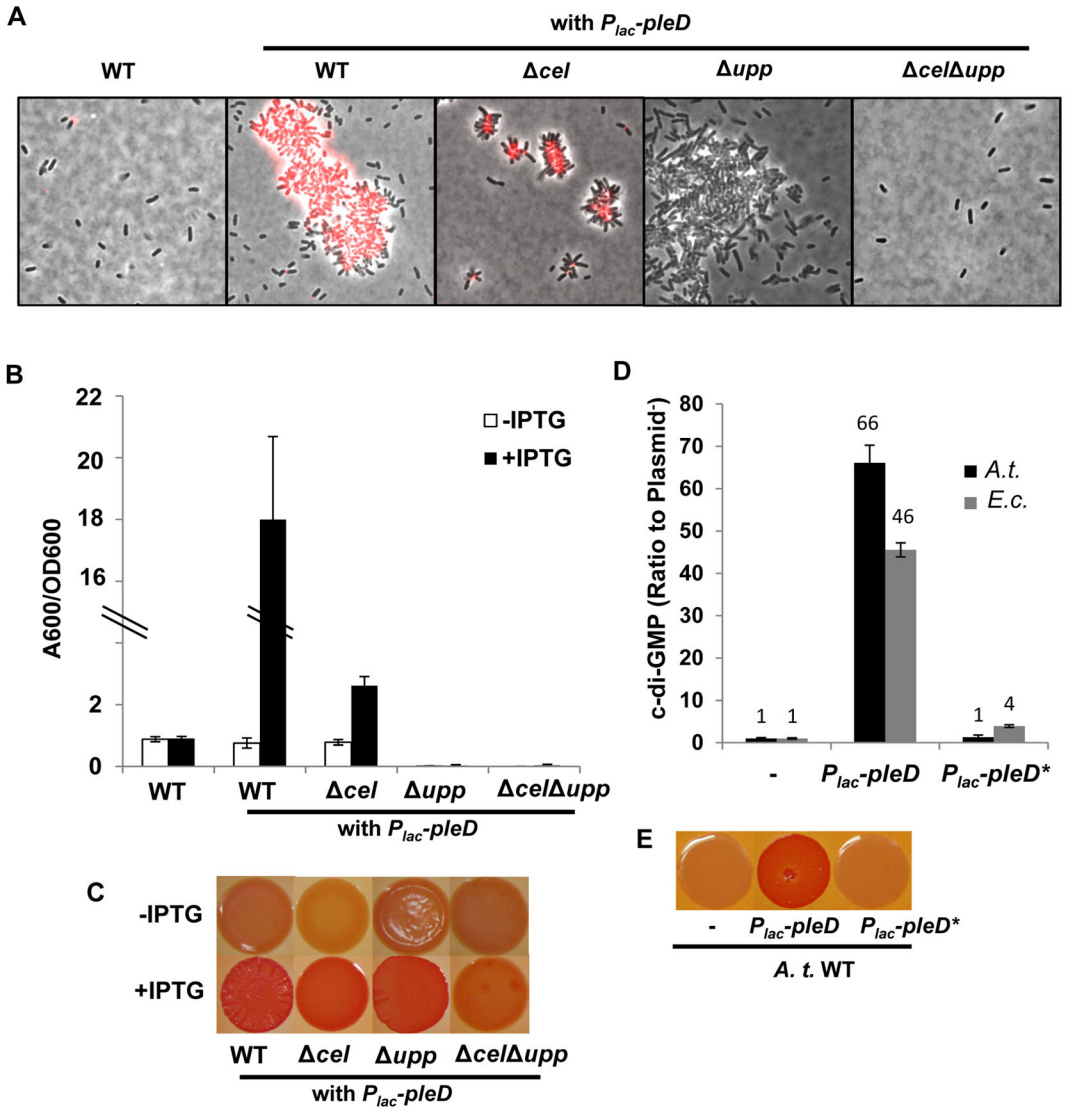

Figure 1. Ectopic expression of *A. tumefaciens pleD* and phenotypic characterization

(A) Fluorescently conjugated WGA lectin (fl-WGA) labeling for UPP elaboration in colonies of *A. tumefaciens* C58 derivatives. Cells were suspended in ddH_2O from fresh colonies of indicated strains on ATGN solid medium plus 0.5 mM IPTG, with or without the IPTG-inducible P_{lac}-*pleD* plasmid. Cells were labeled by AlexaFluor594-WGA and viewed at 100× magnification on a Nikon E800 epifluorescence microscope (excitation, 510–560 nm; emission, >610 nm) and images are an overlay of phase contrast and fluorescence. (B) A quantitative biofilm assay for *A. tumefaciens* C58 derivatives at 48 h. Biofilms formed on PVC coverslips were stained by crystal violet, solubilized in 30% acetic acid and quantified by spectrophotometry at 600 nm. A_{600}/OD_{600} represents the crystal violet quantification A_{600} normalized by culture optical density. White bars indicate cultures grown in ATGN medium without IPTG, and black bars for cultures grown in ATGN medium plus 0.5 mM IPTG. Values are averages of triplicate assays and error bars are standard deviation. (C) Congo Red binding phenotype of *A. tumefaciens* C58 derivatives. Strains harboring the P_{lac}-*pleD* plasmid were grown on ATGN-CR solid media (80 μg/ml Congo Red), with (bottom row) or without (upper row) 0.5 mM IPTG supplementation. Images of the same row were taken from the same plate. (D) Measurement of intracellular levels of c-di-GMP in indicated

strains carrying P_{lac}-*pleD* (wild type plasmid) or P_{lac}-*pleD** (P_{lac}-*pleD* plasmid carrying a GGEEF to GGAAF mutation). *A.t.* (black bars) represents *A. tumefaciens* C58 strain and *E.c.* (grey bars) represents *E. coli* DH5α. The intracellular level of c-di-GMP in either C58 or DH5α strain is normalized to 1. The Y-axis represents the ratio of C58 or DH5α strain harboring a *pleD* expression plasmid to the same strain without a plasmid (50–100 nM for *A. tumefaciens* and 250–500 nM for *E. coli*). Cells at stationary phase were pelleted and resuspended in c-di-GMP extraction buffer containing methanol and acetonitrile. Measurement of c-di-GMP by LC-MS/MS as described in the Methods. Values are averages of triplicate assays and error bars are standard deviation. (E) Congo Red binding phenotype of *A. tumefaciens* C58 strain carrying P_{lac}-*pleD* (wild type plasmid) or P_{lac}-*pleD** (P_{lac}-*pleD* with GGEEF to GGAAF mutation). Colonies were grown on ATGN-CR solid media plus 0.5 mM IPTG. Images were obtained from the same plate.

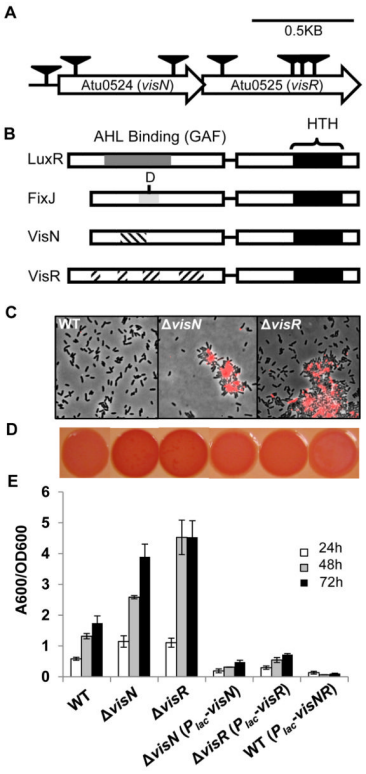

Figure 2. Phenotypic analysis of *visN-visR* mutants isolated from the ECR genetic screen

(A) Genetic map and transposon insertions in *visN* (Atu0524) and *visR* (Atu0525) genes. Transposon mutants were isolated from a ($EPS^{-}UPP^{+}$) parent strain, an *A. tumefaciens* C58 derivative deficient in all major exopolysaccharides except for UPP. Triangles indicate transposon insertion sites isolated from independent transposon insertion events from a genetic screen for 25,000 colonies. (B) Comparison of the domain structures of LuxR and FixJ family proteins with the putative domains of VisN and VisR proteins from *A. tumefaciens*. Black boxes represent Helix-Turn-Helix (HTH) DNA binding motifs. The dark grey shade represents the acylhomoserine lactone (AHL) binding domain or GAF domain of LuxR-type proteins, the light grey domain represents the conserved receiver domain of FixJ-type proteins, with the conserved aspartic acid residue indicated, and the hatched regions represent the conserved residues of VisN and VisR proteins among different rhizobia. (C) Labeling with fl-WGA lectin for UPP elaboration in planktonic cultures of indicated *A. tumefaciens* C58 derivatives. Cells at exponential phase (OD_{600} 0.6~0.8) were labeled by fl-WGA and viewed at 100× magnification on a Nikon E800 epifluorescence microscope (excitation, 510–560 nm; emission, >610 nm) with an overlay of phase contrast and fluorescence images. (D) Congo Red binding phenotypes of indicated *A. tumefaciens* C58 derivatives as labeled in panel E. Strains were grown on ATGN-CR solid medium plus 0.5 mM IPTG. (E) A quantitative biofilm assay plotting solubilized crystal violet staining (A_{600}) normalized to culture OD_{600} by the indicated *A. tumefaciens* derivatives at 24 h, 48 h and 72 h as in Fig. 1B. All strains were grown in ATGN medium plus 0.5 mM IPTG. Values are averages of triplicate assays and error bars are standard deviation.

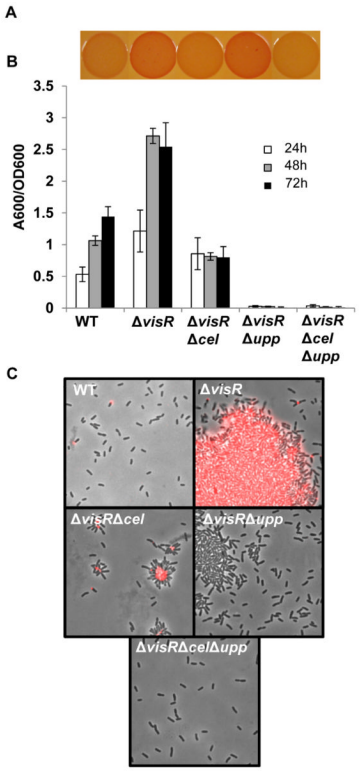

Figure 3. The Δ*visR* mutant is elevated for UPP and cellulose production

(A) Congo Red binding phenotypes of indicated *A. tumefaciens* C58 derivatives as in Fig. 1C. (B) A quantitative biofilm assay plotting solubilized crystal violet staining (A_{600}) normalized to culture OD_{600} by the indicated *A. tumefaciens* derivatives at 24 h, 48 h and 72 h as in Fig. 1B. All strains were grown in ATGN medium. Values are averages of triplicate assays and error bars are standard deviation. (C) Labeling with fl-WGA lectin for UPP elaboration in colonies of indicated strains as described in Fig. 1A.

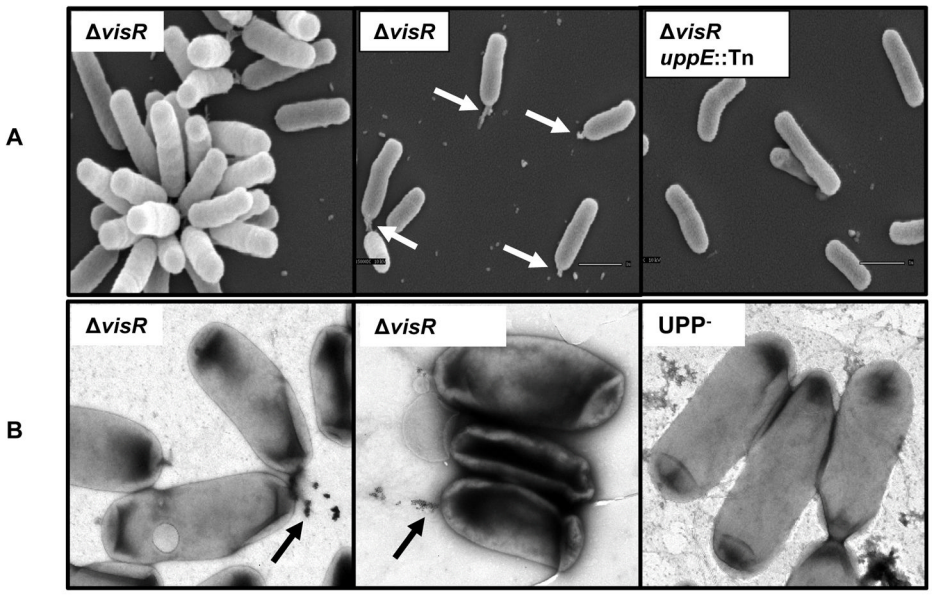

Figure 4. Visualization of UPP by electron microscopy

(A) Visualization of UPP by scanning electron microscopy. Indicated strains were Δ*visR* mutant in the EPS^{-}UPP^{+} backgrounds. The *uppE*::Tn represents a Mariner transposon insertion in the *uppE* gene required for UPP biosynthesis. Bacterial cells on coverslips were fixed by glutaraldehyde, and after processing sputter coated with gold before observation using JEOL JSM-5800 LV Scanning Electron Microscope at 10 kV. White arrows indicate unipolar material. (B) Visualization of UPP by transmission electron microscopy for the Δ*visR* mutant in the EPS^{-}UPP^{+} backgrounds. The UPP^{-} strain was *uppA-F* in-frame deletion mutant constructed in an otherwise wild type background. Cells were labeled with colloidal gold conjugated WGA, stained by uranyl acetate and observed on carbon-coated grids. Black arrows indicate the colloidal gold conjugated WGA labeled polar material.

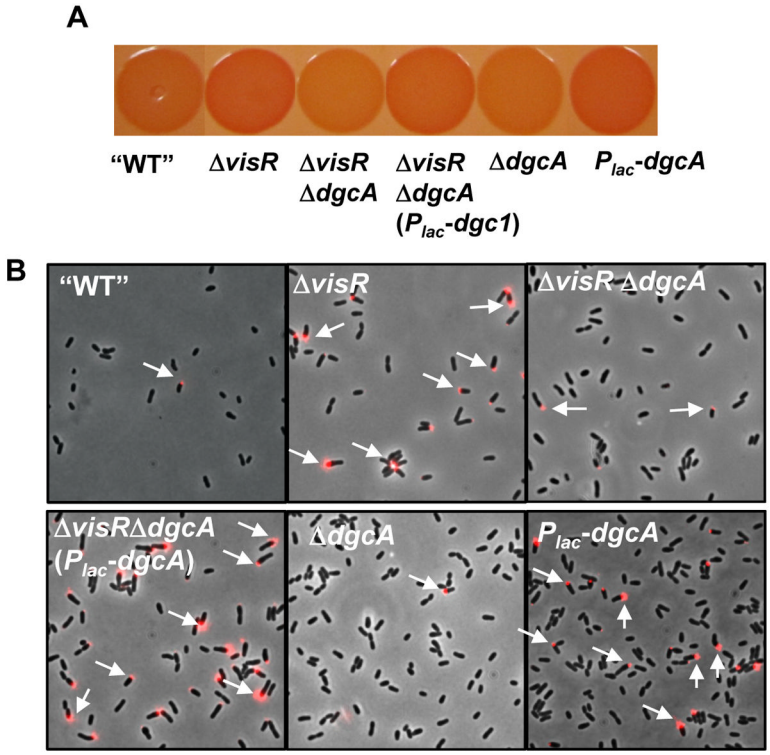

Figure 5. Isolation of the putative GGDEF gene *dgcA* from a DCR suppressor screen

(A) Congo Red binding phenotype of indicated *A. tumefaciens* C58 derivative grown on ATGN-CR solid media plus 0.5 mM IPTG, as in Fig. 1C. All strains were constructed in $EPS^{-}UPP^{+}$ background. In this figure "WT" refers to the $EPS^{-}UPP^{+}$ strain. (C) Labeling with fl-WGA lectin for UPP production in colonies of the indicated derivatives from ATGN agar plus 0.5 mM IPTG as in Fig. 1A. Arrows highlight lectin labeling on cell poles. All strains were constructed in $EPS^{-}UPP^{+}$ background, and "WT" refers to this strain.

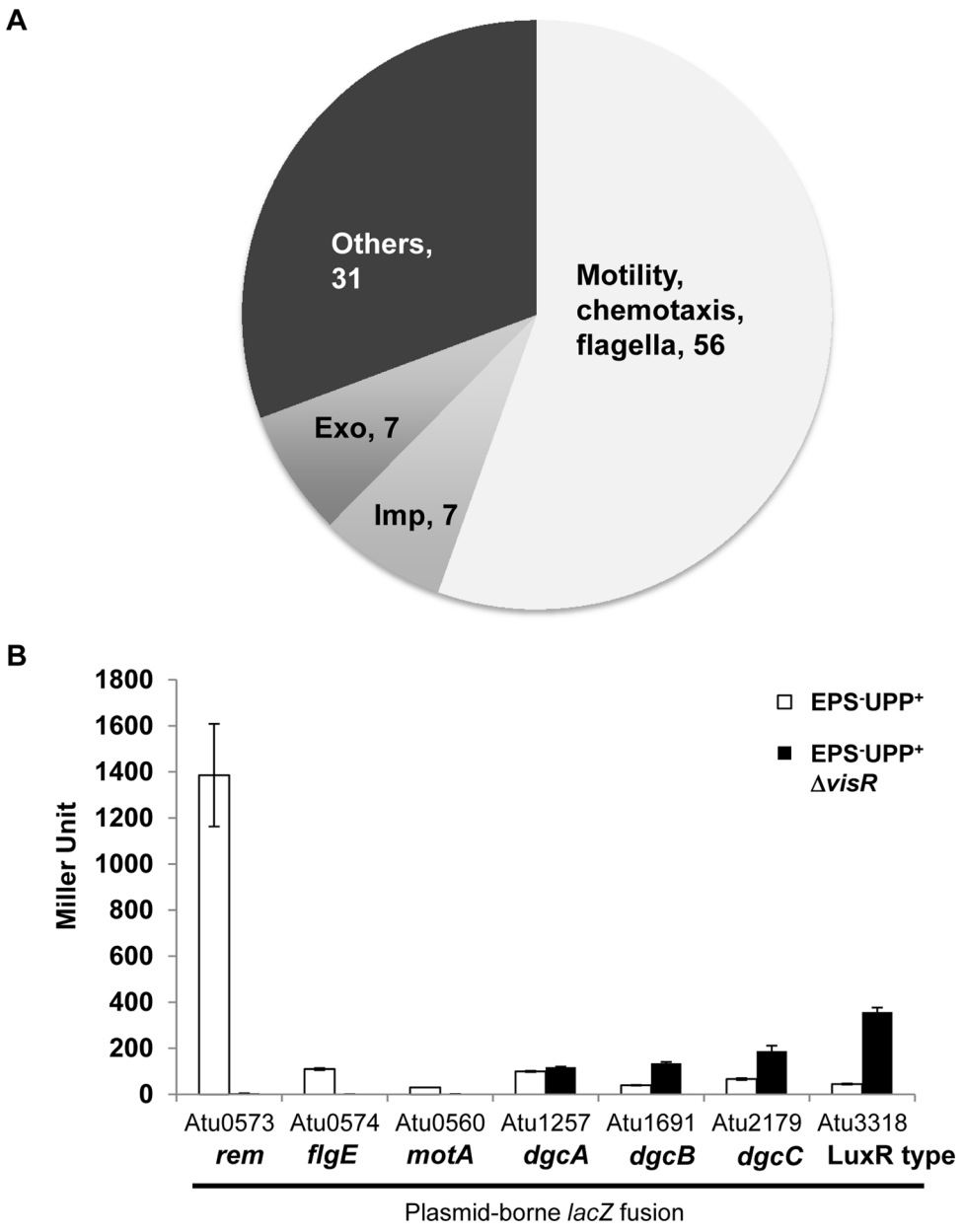

Figure 6. Identification of VisR regulon by DNA microarray

(A) Pie chart showing the classification and number of genes with decreased expression in the *A. tumefaciens* Δ*visR* mutant as determined by Agilent DNA microarrays from 4 biological replications and 2 dye swaps. Genes with a t-test P-value < 0.05 and with $\log_2$ ratios more negative than −0.6 (representing a fold-change of −1.5) are graphed. (B) β galactosidase specific activity plotting Miller Units from ATGN grown cultures of *A. tumefaciens* $EPS^{-}UPP^{+}$ strain (white bars) and the $EPS^{-}UPP^{+}$Δ*visR* mutant (black bars) harboring the indicated plasmid-borne *lacZ* translational fusions. Values are averages of triplicate assays and error bars are standard deviations.

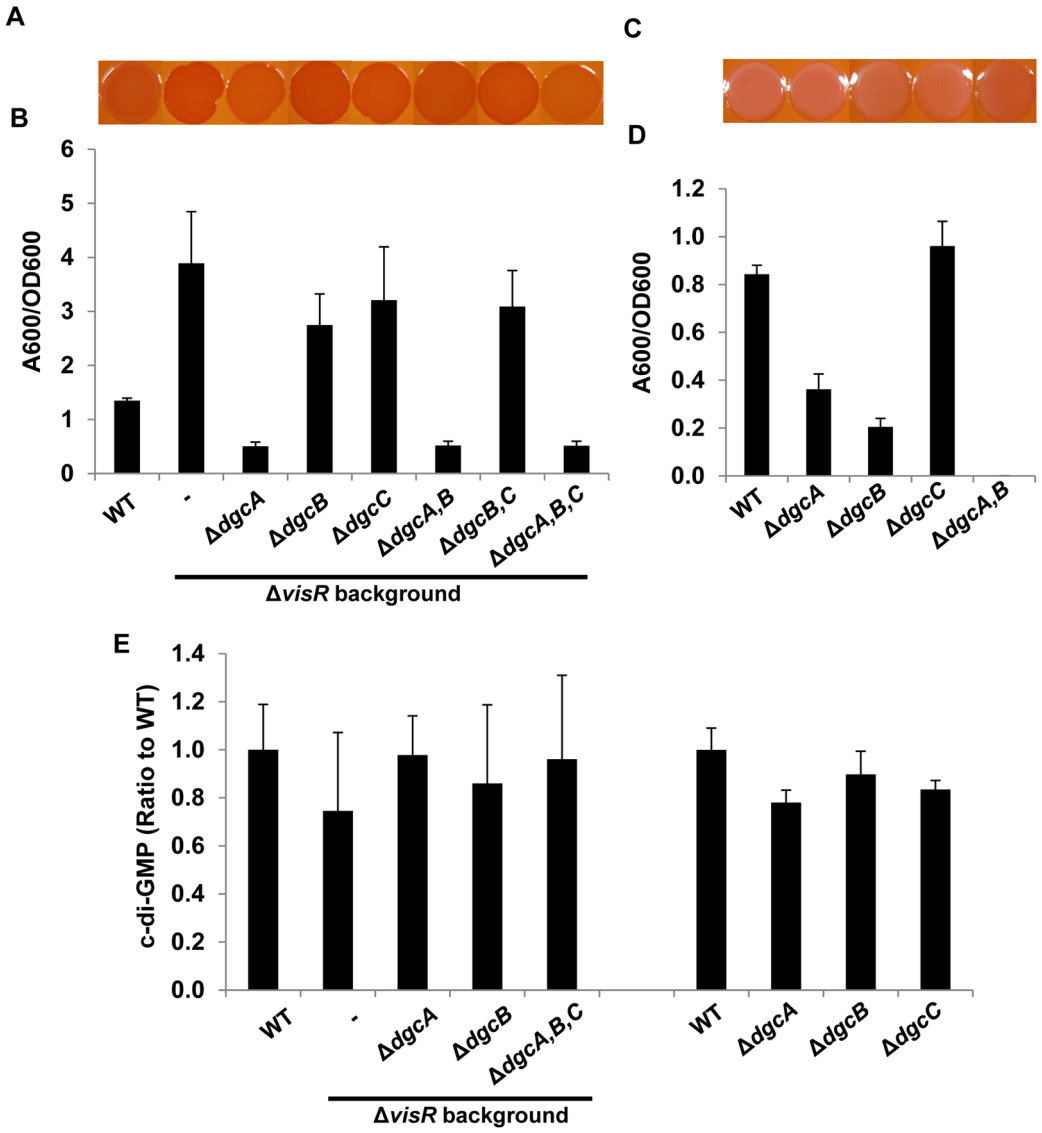

Figure 7. Phenotypic analysis of *dgcA*, *dgcB* and *dgcC* mutants and their contributions to the *visR* phenotype

(A) and (C) Congo Red binding phenotypes of indicated *A. tumefaciens* C58 derivatives as described in Fig. 1C. (B) and (D) Quantitative biofilm assay plotting solubilized crystal violet staining (A_{600}) normalized to culture OD_{600} at 48 h as described in Fig. 1B. All strains were grown in ATGN medium. Values are averages of triplicate assays and error bars are standard deviation. (E) Measurement of intracellular levels of c-di-GMP in indicated *A. tumefaciens* C58 derivatives, as described in Fig. 1D. Levels of c-di-GMP for C58 wild type are 50–100 nM and the value for each mutant is represented as a ratio to those measured for the wild type.

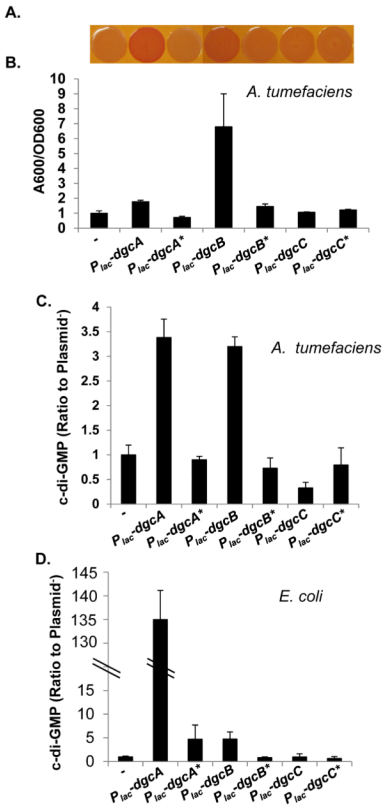

Figure 8. Site-directed mutants of putative catalytic sites of DgcA, DgcB and DgcC

(A) Congo Red binding phenotype of *A. tumefaciens* C58 wild type strain carrying plasmids as labeled in panel B. All strains were grown on ATGN-CR solid medium plus 0.5 mM IPTG. (B) A quantitative biofilm assay (48 h) for *A. tumefaciens* C58 wild type strain carrying plasmids as indicated. Cultures were grown in ATGN medium plus 0.5 mM IPTG. Values are averages of triplicate assays and error bars are standard deviation. Plasmids carrying GGEEF to GGAAF site-specific mutations are indicated with an asterisk (*). (C) Measurement of intracellular level of c-di-GMP in *A. tumefaciens* C58 strain carrying the indicated plasmid, as described in Fig. 1D. Cultures were grown in ATGN medium plus 0.5 mM IPTG. The Y axis represents the ratio of the C58 strain carrying a DGC expression plasmid to the same strain without a plasmid (50–100 nM). (D) Measurement of intracellular levels of c-di-GMP in *E. coli* DH5α carrying the indicated plasmid, as described in Fig. 1D. Cultures were grown in LB medium plus 0.5 mM IPTG. The intracellular level of c-di-GMP of *E. coli* DH5α strain is 250–500 nM and normalized to 1. The Y axis represents the ratio of *E. coli* DH5α strain carrying a plasmid to the same strain without a plasmid.

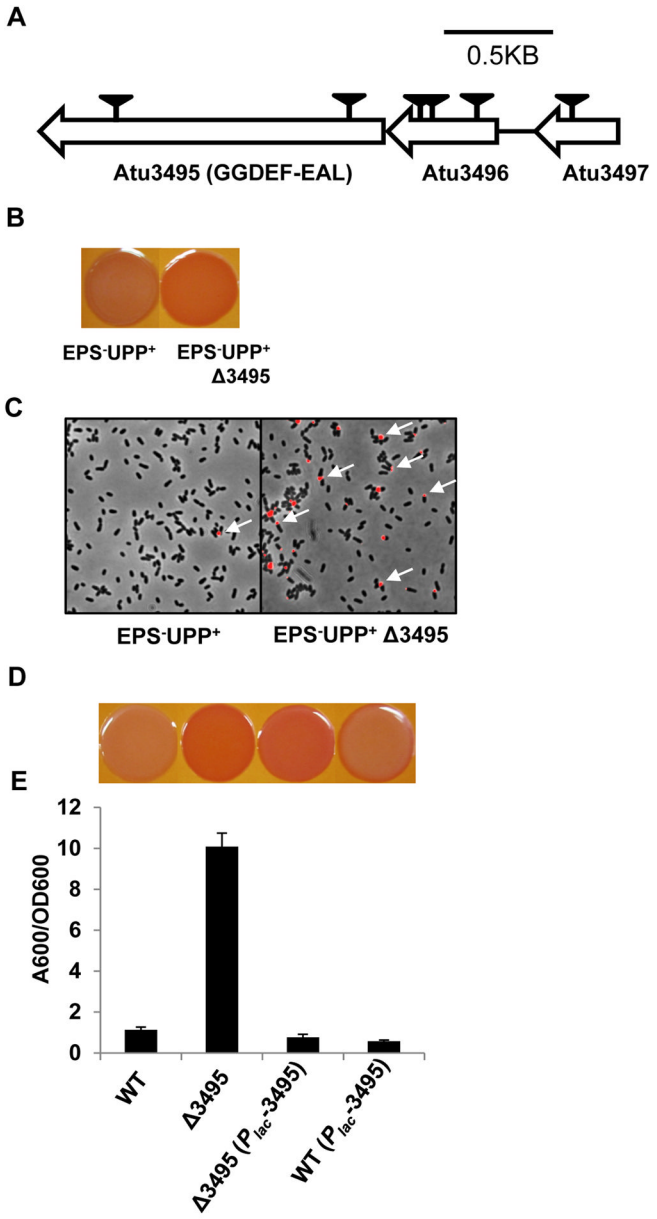

Figure 9. Phenotypic analysis of the putative phosphodiesterase Atu3495

(A) Genetic map and transposon insertions in Atu3495–Atu3497 genes. Transposon mutants were isolated from a ($EPS^{-}UPP^{+}$) parent strain, deficient in all major exopolysaccharides except for UPP. Triangles indicate transposon insertion sites isolated from independent transposon insertion events. (B) Congo Red binding phenotype of indicated strains, as described in Fig. 1C. (C) Labeling with fl− WGA lectin for UPP elaboration in colonies, as indicated in Fig 1A. (D) Congo Red binding phenotypes of *A. tumefaciens* C58 derivatives as labeled in panel E, and all grown on ATGN-CR solid media plus 0.5 mM IPTG. (E) A quantitative biofilm assay plotting solubilized crystal violet staining (A_{600}) normalized to culture OD_{600} by the indicated *A. tumefaciens* derivatives at 48 h, as described in Fig. 1B. All strains were grown in ATGN medium plus 0.5 mM IPTG. Values are averages of triplicate assays and error bars are standard deviation.

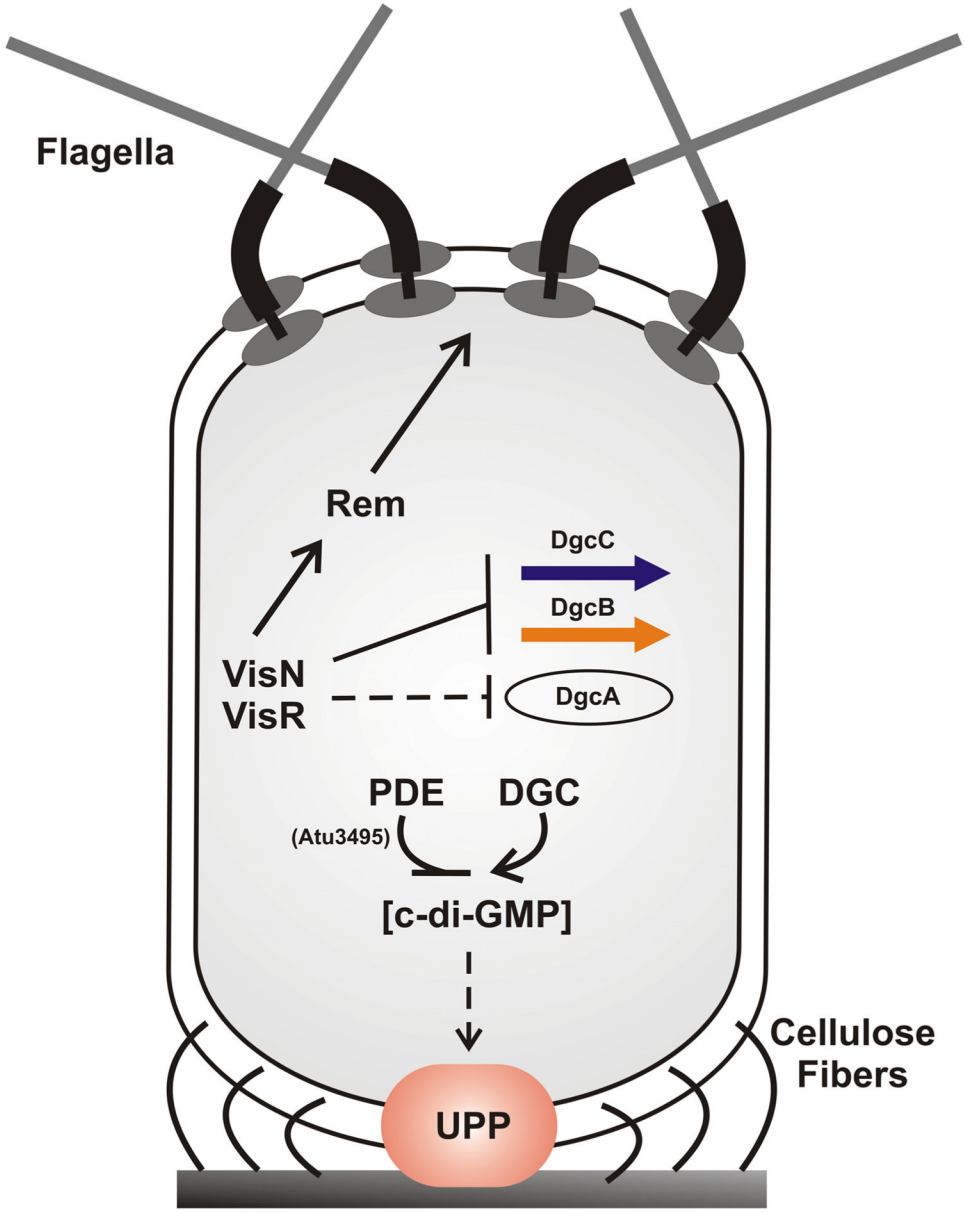

Figure 10. Working model of VisN-VisR and c-di-GMP regulation of motility and polysaccharide synthesis

The turnover of c-di-GMP, which is controlled by phosphodiesterase EAL proteins and diguanylate cyclase GGDEF proteins, positively regulates the production of UPP (indicated by orange ellipse) and cellulose fibers (indicated by the curved lines). Cells with elevated c-di-GMP elaborate the UPP independent of surface contact. VisNR negatively regulates UPP and cellulose through modulating the c-di-GMP levels via the diguanylate cyclases DgcA, DgcB and perhaps DgcC. VisN-VisR directly or indirectly regulates the transcription of *dgcB* and *dgcC*, while directly or indirectly regulating *dgcA* post-transcriptionally. VisNR regulates motility and flagellar function through the Rem transcriptional activator, as in *S. meliloti*.